Development of Test Bench for Transfemoral Prosthesis

Author

MUHAMMAD ZAWAR UL HASSAN

00000204012

Supervisor

DR. MOHSIN ISLAM TIWANA

DEPARTMENT OF MECHATRONICS ENGINEERING

COLLEGE OF ELECTRICAL & MECHANICAL ENGINEERING

NATIONAL UNIVERSITY OF SCIENCES AND TECHNOLOGY

ISLAMABAD

AUGUST 2021

Development of Test Bench for Transfemoral Prosthesis

Author

MUHAMMAD ZAWAR UL HASSAN

00000204012

MS-17

A thesis submitted in partial fulfillment of the requirements for the degree of

MS Mechatronics Engineering

Thesis Supervisor:

DR. MOHSIN ISLAM TIWANA

Thesis Supervisor's Signature: _____

DEPARTMENT OF MECHATRONICS ENGINEERING

COLLEGE OF ELECTRICAL & MECHANICAL ENGINEERING

NATIONAL UNIVERSITY OF SCIENCES AND TECHNOLOGY,

ISLAMABAD

AUGUST 2021

Declaration

I certify that this research work titled "*Development of Test Bench for Transfemoral Prosthesis"* is my own work. The work has not been presented elsewhere for assessment. The material that has been used from other sources it has been properly acknowledged / referred.

Signature of Student

Muhammad Zawar Ul Hassan

00000204012

Language Correctness Certificate

This thesis has been read by an English expert and is free of typing, syntax, semantic, grammatical and spelling mistakes. Thesis is also according to the format given by the university.

Signature of Student
Muhammad Zawar Ul Hassan
00000204012

Signature of Supervisor
Dr. Mohsin Islam Tiwana

Copyright Statement

- Copyright in text of this thesis rests with the student author. Copies (by any process) either in full, or of extracts, may be made only in accordance with instructions given by the author and lodged in the Library of NUST College of E&ME. Details may be obtained by the Librarian. This page must form part of any such copies made. Further copies (by any process) may not be made without the permission (in writing) of the author.

- The ownership of any intellectual property rights which may be described in this thesis is vested in NUST College of E&ME, subject to any prior agreement to the contrary, and may not be made available for use by third parties without the written permission of the College of E&ME, which will prescribe the terms and conditions of any such agreement.

- Further information on the conditions under which disclosures and exploitation may take place is available from the Library of NUST College of E&ME, Rawalpindi.

Acknowledgements

I am thankful to my Creator Allah Subhana-Watala to have guided me throughout this work at every step and for every new thought which He setup in my mind to improve it. Indeed, I could have done nothing without His priceless help and guidance. Whosoever helped me throughout the course of my thesis, whether my parents or any other individual was His will, so indeed none be worthy of praise but Him.

I am profusely thankful to my beloved parents who raised me when I was not capable of walking and continued to support me throughout in every department of my life.

I would also like to express special thanks to my supervisor Dr. Mohsin Islam Tiwana for his help throughout my thesis.

I would also like to thank Dr. Amir Hamza and Dr. Waqar Shahid Qureshi for being on my thesis guidance and evaluation committee.

Finally, I would like to express my gratitude to all the individuals who have rendered valuable assistance to my study.

Dedicated to my exceptional parents and adored siblings whose tremendous support and cooperation led me to this wonderful accomplishment

Abstract

Rapid prototyping and standardizing play a crucial part in manufacturing prosthesis and meet emerging demand of modern time. Testing procedures involving human subjects involves safety and legal complications that tends to introduce time delays reducing the productivity and quality of prosthesis. This thesis involves development of 2 DOF transfemoral prosthesis testing platform for cyclic testing considering hip vertical motion and thigh horizontal motion. The system is simulated to evaluate the torque required for the hip motions and fabricated to replicate human hip vertical motion and thigh rotational motion. Furthermore, Moreover, cyclic durability testing using FEM technique is performed on foot prosthesis for future fabrication and testing on prosthesis test bench.

Key Words: *Test Bench, Transtibial Prosthesis, Transfemoral Prosthesis, Cyclic Testing, Fatigue testing, FEM technique, cyclic durability testing.*

Table of Contents

List of Figures

List of Tables

CHAPTER 1: INTRODUCTION

During recent decades, statistics show huge increase in amputees worldwide majorly due to alarming increase in patients of cardiovascular disease (especially diabatic patients), trauma, malignancy and congenital limb defects [1][2]. The cause of limb amputation varies region wise: Low- and Middle-Income countries (LMIC s) registers trauma as primary cause of amputation [3][4][5], whereas peripheral vascular disease and diabetes is registered as root cause of amputation in High Income Countries (HICs) [6][7][8]. According to a study, 57.7 million people have suffered from limb amputation from a traumatic cause world-wide since 2017 of which 35.3 million faced lower limb amputation. Four leading traumatic cause of limb amputation had been found including falls (36.2%), road accidents (15.7%), mechanical force (10.4%) and transportation (11.2%) [9][10][11]. In Pakistan, According to PWDs, 5.035 million people have gone through amputations having annual growth rate of disabilities increase to 2.65% per annum; the numbers are higher than developed countries.

The level of amputation depends on which tissue is required to be removed, incision and how well the residual limb is functioning [12]. Commonly observed lower limb amputation level can be divided into two major groups: Transfemoral lower limb amputation (amputation above knee) and transtibial lower limb amputation (knee remains intact). For transfemoral amputees, above knee prosthesis is developed including knee and ankle prosthesis attached to the upper and lower shanks and foot, respectively. Whereas for transtibial prosthesis, below-knee prosthesis is developed which includes shanks connected to ankle/foot prosthesis that is further linked to an elastomer foot [13].

The safety of both types of prosthesis is ensured by two international standards that are ISO-10328:2016 and ISO-22675:2016. ISO-10328:2016 deals in structural testing of lower limb prosthesis and ISO-22675:2016 deals with the cyclic durability testing and performance analysis of ankle-foot prosthesis[14]. These tests can be conducted using Finite Element method in a virtual environment reducing the development time and cost of the prosthesis however real-time verification provides authenticity to the durability and strength of material used for manufacturing [15] [16] [17].

Considering increasingly demand of lower limb prosthesis, rapid manufacturing of prosthesis with enhanced quality assurance and quality control is a requirement of modern age. The in-vivo testing methods, having direct involvement of an amputee and reliance on contribution and his opinion, involves time delays and legal clearance issues. Furthermore, it

considers safety harness and involves lack of gait repeatability which restricts the testing scope and quality of data extracted from prosthesis under observation. Ultimately the production rate is slowed and leads to slow advancements in this field [18].

A robotic testing method is required that may reduce the obstacles comprehended in testing phase and reduce the production time. It can help simulate unbounded situations including near-fall scenarios that is unrecommended while testing through mounting prosthesis to an amputee [18]. It can provide continuous sequential motion to verify endurance of the prosthesis as well as real-time optimization of control algorithms. Furthermore, sensors mounted on a robot produces better results during simulations while measuring tedious quantities; hip and knee motions and torques. Robots can compare different designs available in the market and can be a decisive tool in understanding and evaluating prosthesis for any state of amputee; this is possible only under controlled test parameters and conditions having enough trail datasets[19].

This thesis deals with design and fabrication of Test Bench for transfemoral prosthesis. The remainder of thesis chapters are summarized as follows:

Chapter 2: Deals in literature review regarding the previously conducted test benches

Chapter 3: Design and fabrication of test bench

Chapter 4: Cyclic testing using FEA technique

Chapter 5: Conclusion and Future Work

Annexures

References

CHAPTER 2: LITERATURE REVIEW

Human body can be bisected using three anatomical planes that are Sagittal Plane, frontal Plane and Transverse Plane as shown in fig 2-1(a) [20]. These planes help in defining the biomechanics of ankle, knee, and hip joint motions in three different aspects. These joint motions are commonly categorized as extension, flexion, eversion, inversion, adduction, abduction and dorsi-flexion and plantar flexion in case of ankle motion in sagittal planes as shown in fig 2-1(b).

2.1 Anatomy of Lower Limb

Human locomotion is performed using coordination of lower limb anatomical structures including pelvis, hip joint, knee joint and ankle joint. The anatomical study of these portion and their role in human gait is necessary to develop an optimum lower limb prosthetic device. Hip joint can be classified as ball-and-socket synovial joint formed by the union of acetabulum and head of femur [21]. Ball and socket nature corresponds to motion of hip joint in all three anatomical planes. These movements can be classified as flexion and extension of hip in sagittal plane, abduction, adduction in coronal plane and medial and lateral rotation in transverse/horizontal plane. The average angular displacement for sagittal plane is 20 degrees in extension and 120 degrees in flexion. Similarly, 40 degrees of angular movement in abduction and 30 degrees of movement in internal and external rotation in frontal and horizontal plane is reported.

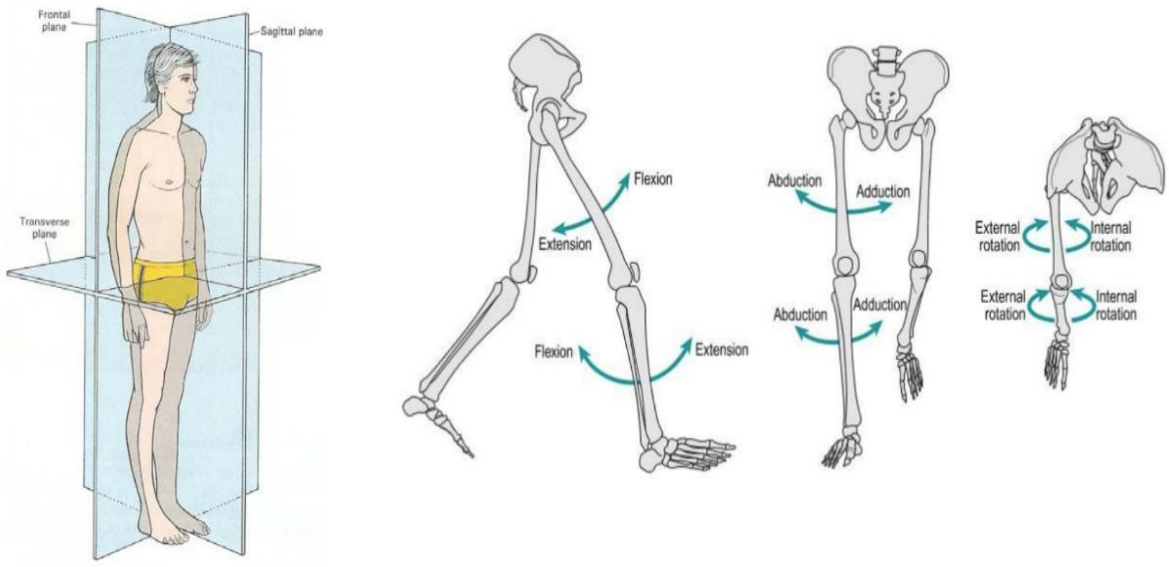

Figure 2-1 (a)Anatomical Planes bisecting a human body (b) movement of lower limb [20]

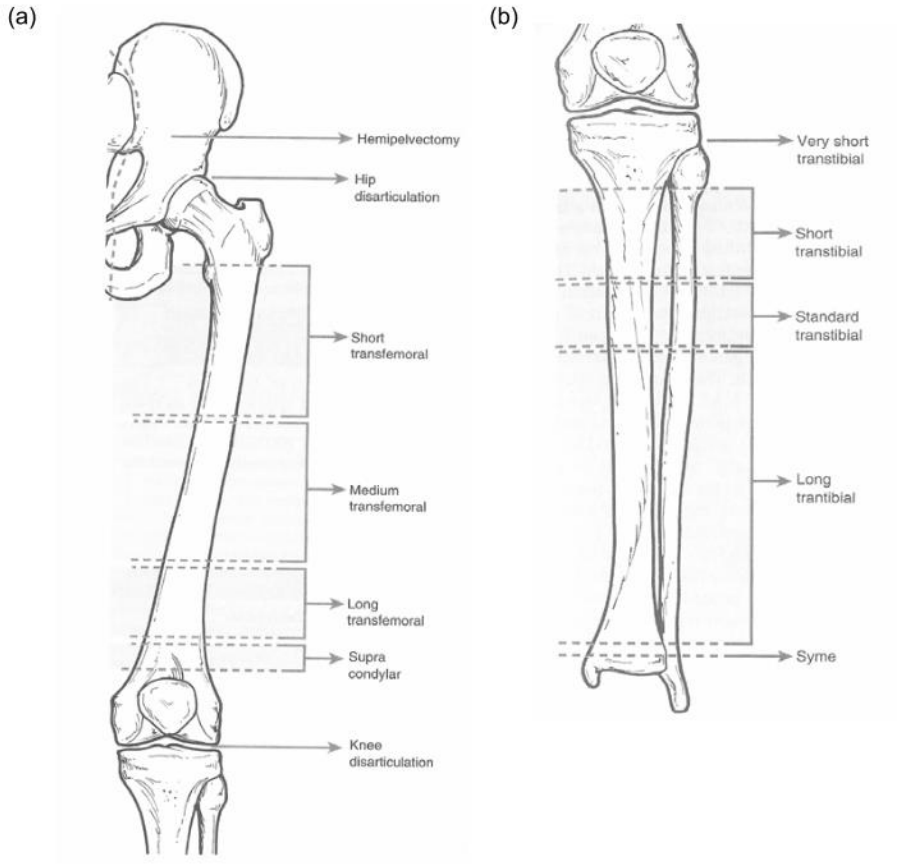

Figure 2-2 Lower limb anatomy [20]

Knee joint comprises of two complex joints having motion in sagittal and transverse planes: tibiofemoral and patellofemoral joints. The knee motion performs key functions such as controlling the flexion/stride in swing phase and absorbing shock and transmitting force during stance phase [22].

Human ankle is large joint comprises three vital bones: shin, thinner and foot bones. These bones provide support to the whole body during human gait and provide motion to the foot. Six joint motions can be perform using human ankle and foot which are termed as extension, flexion, eversion, inversion, dorsi-flexion, and plantar flexion. The joint angles reduce in flexion and increase in extension as shown in figure 2-3(a). Plantar flexion and dorsi flexion movement of foot takes place in sagittal plane wherein joint angle is decrease while dorsi flexion movement and increases during plantar flexion as indicated in figure 2-3(b). Foot inner movement is considered eversion and outward movement is considered inversion as indicated figure 2-3(c) [20][23]

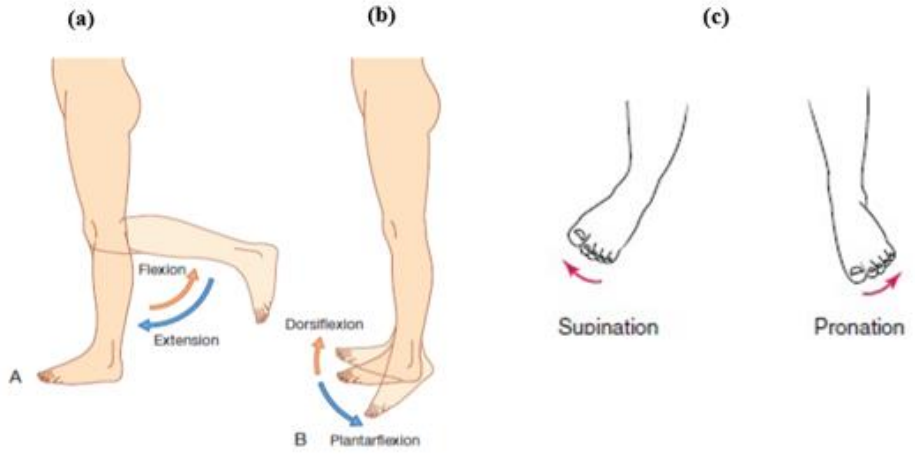

Figure 2-3 (a) Movement of tibia in sagittal plane (b) movement of ankle/foot in sagittal plane (c) movement of foot in frontal plane [20]

2.2 Basic Features of Walk

Walking is categorized as a complex phenomenon for examination and replication considering the complex cyclic repetition of the strides and balancing of human upper portion including torso, upper limbs, and head as well as lower extremities. To understand the movements of the anatomical structure, the best possible way is to understand the biochemical signals generated from the movement of portion under consideration. However, the movements can also be monitored and observed through internal, external, and inertial forces exerted on or from the joints[24].

Human body can be segregated into two segments: the passenger and the locomotor. The upper portion including the torso, arms and hands, neck and head can be considered as passenger part whereas the legs including hip joints, thighs, knees, and foot are considered locomotor of the body. Moreover, each portion of the body participates in producing the movements such that the motions are interlinked to achieve best results. For example, the synchronized movements of upper limbs help in reducing the energy conservation of whole body whereas it does not participate in the movement and balancing of the body. This provides the opportunity to analyze the mechanics of locomotor separately from the passenger portion if energy consumption is not considered. This also concludes that any disorder in lower limb prosthesis has direct consequences on the gait pattern of human being and the behavior of the locomotor can be replicated separately without considering the behavior of whole body [25].

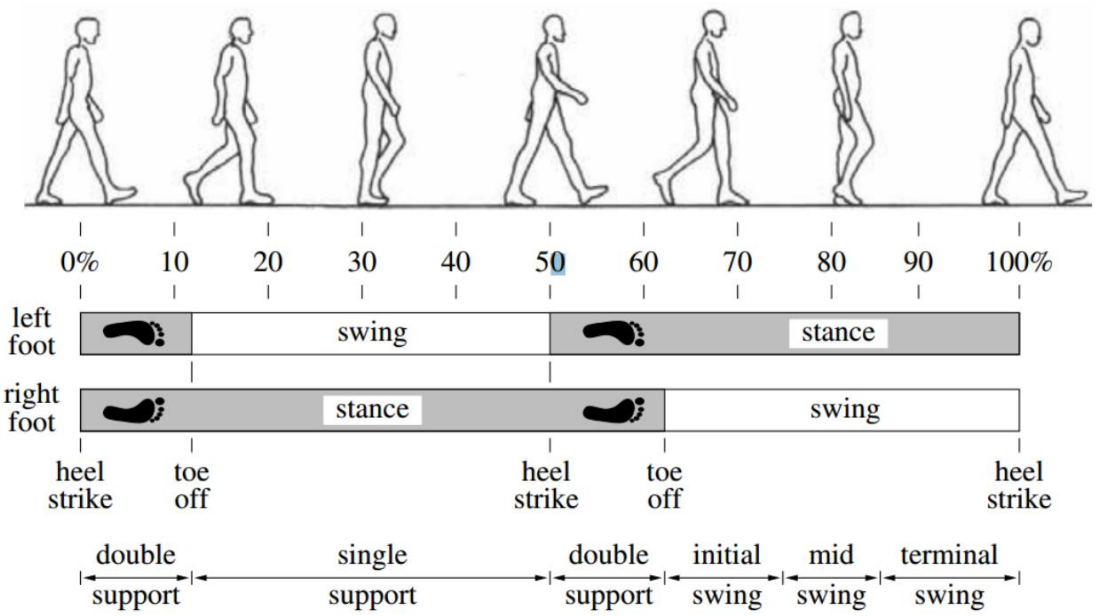

Figure 2-4 Gait cycle for human locomotion [24]

The synchronized sequence of movement of these parts made up the gait cycle which can broadly be divided into two main phases: stance and swing phase. The stance and swing phase divide and represent 60% and 40% of gait cycle, respectively. Two steps taken synchronously one after another constitutes a stride. Furthermore, the stance phase and swing phase are divided into seven different phases as listed in table 2-1 [26].

2.3 Lower Limb Prosthesis

Prosthesis is a device that aims to replicate the shape and functionality of the missing/defected anatomical structure. Lower limb amputation can be categorized in two major regions that are below knee amputation and above knee amputation. Below knee amputation can be segregated as amputation having knee joint intact with the residual limb and a missing ankle and foot. In above knee amputation, amputation is performed on thigh portion extricate the knee, tibia, ankle, and foot area. The prosthesis designed to cover below knee amputation is stated as Transtibial Prosthesis (TT). TT prosthesis is fabricated using below knee socket, pylon, ankle joint and developed foot. For above knee amputation, Transfemoral Prosthesis (TF) is designed which includes socket, knee joint, pylon, ankle joint and fabricated foot. Both prostheses are illustrated in figure 2-4.

Table 2-1 Detailed characteristics of human walk

Gait Analysis.					
Stance Phase					
Time	**Hip/femur Movement**	**Knee / tibia movement**	**Ankle Movement**	**Support**	**Description**
Initial Phase (0%)	Flexion	Extension	Dorsi-Flexion to neutral position	Initial Contact Double support	Initial Contact Heel touch the ground Opp. Leg completes support phase Starts with heel strike of leading foot and end at toe leaving of lagging foot
Loading Response (0% - 10%)	Flexion to Extension	Flexion	Plantar-Flexion	Single Support	Lowest position of trunk Body weight shifted to double support Shock absorption followed by body weight shifting and forward motion.
Midstance (10% - 30%)	Extension	Extension	Dorsal-Flexion	Single Support	Tenure from lagging foot toe-off to leading foot heel-off Trunk reaches highest point Center of mass aligned to ball of foot
Terminal Stance (30%-50%)	Extension increases	Max. extension at heel rise	Dorsal-Flexion at heel rise	Single Support	Tenure from start of heel-off of leading foot to heel strike of lagging foot Body transferred beyond vertical axis Trunk starts sinking
Pre-swing (50%-60%)	Extension decreases	Flexion	Plantar-Flexion	Double Support	Tenure of lagging foot heel-off to toe-off Transfer of weight to leading another limb
Swing Phase					
Initial Swing (60% - 75%)	Flexion increases	Flexion increases	Partial Dorsal Flexion	Single Support	Tenure from lagging foot leaving the ground to swing limb aligned to support limb
Mid Swing (75% - 90%)	Flexion	Extension due to gravitational	Dorsal Flexion to neutral	Single Support	Swing continues until fibula is vertically aligned to adjacent limb

		force	position		
Step Termination (90% 100%)	Flexion	Extension	Dorsal Flexion to neutral position	Single Support	Starts with swing leg fibula in vertical position to heel strike on the ground

2.4 Components of lower limb prosthesis

Lower limb Prosthesis can be classified as assembly of following listed parts.

Socket: The residual limb portion is attached to the prosthesis part using custom made sockets designed according to the shape and of limb potion. It is crucial to design the socket precisely as it transfers whole-body weight and forces and torques generated during walking phase.

Knee Prosthesis: Knee prosthesis provides connection of socket to transtibial portion allowing the lower limb to flex and extend in accordance with the walking requirement. It provides static stability to the lower limb portion and endures the dynamic responses generated during walking.

Pylon: a standard 30mm diameter pylon provides connection between ankle and knee joint.

Foot and Ankle System: Foot ankle system is source of interaction of whole body to the ground[20].

Engineers and scientists have developed various knee and ankle/foot prosthesis that tends to meet the amputees' requirement. The selection and assignment of prosthesis is done on following listed factors using patient history and physical conditions.

1. Patients physical and mental scenario
2. Anthropometric measures
3. Level of amputation
4. Disease
5. Age of amputee
6. Activity level of amputee
7. Environmental conditions
8. Advancement in technology

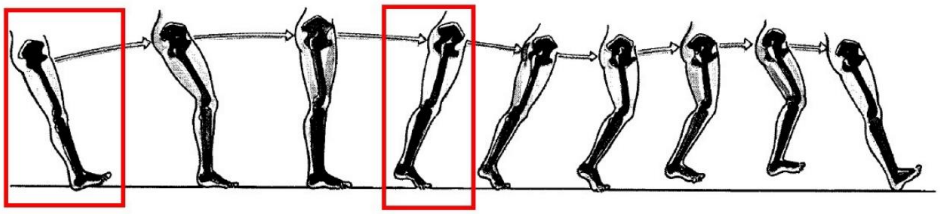

Figure 2-5 Maximum loading posture during gait cycle [24]

2.5 Legislation in force

Standards and experimental procedures are developed by the scientists and engineers to test mechanical strength and endurance and performance testing of lower limb prosthesis in real-time usage. ISO10328:2016 and ISO 22675:2016 have been developed as a guideline perform strength and performance testing of fabricated prosthesis.

ISO 10328:2016 - "Prosthesis – structural testing of lower limb prosthesis" deal in mechanical strength and endurance tests of lower limb prosthesis

ISO 22675:2016 – "Prosthetics — Testing of ankle-foot devices and foot units — Requirements and test methods" deal in mechanical strength and endurance tests of ankle foot prosthesis along with performance testing.

Following aspects are covered in the document.

1- Definition, identification, selection, and preparation of test samples
2- Designation of the test categories
3- Configuration of experimental setups
4- Description of test loading conditions and test loading samples
5- Specifications of test equipment compliance
6- Execution of the experimental procedures
7- Verification of the performance requirements fulfilment

The document aims to ensure suitable strengths endured by the prosthesis is testing during usage. It is evident that the prosthesis experience complex loading at different load axis during use by an amputee and multiple test procedures are required to fulfill the strength test criteria. Hence, the standard segregates the test procedure considering maximum loading against two different phases in accordance with the gait analysis performed by the researchers. Each test has its own configuration and loading criteria and nodes where maximum likelihood of stress and strains may be present.

Condition A: maximum loading occurring early stance phase.

Condition B: maximum loading occurring late stance phase. [24]

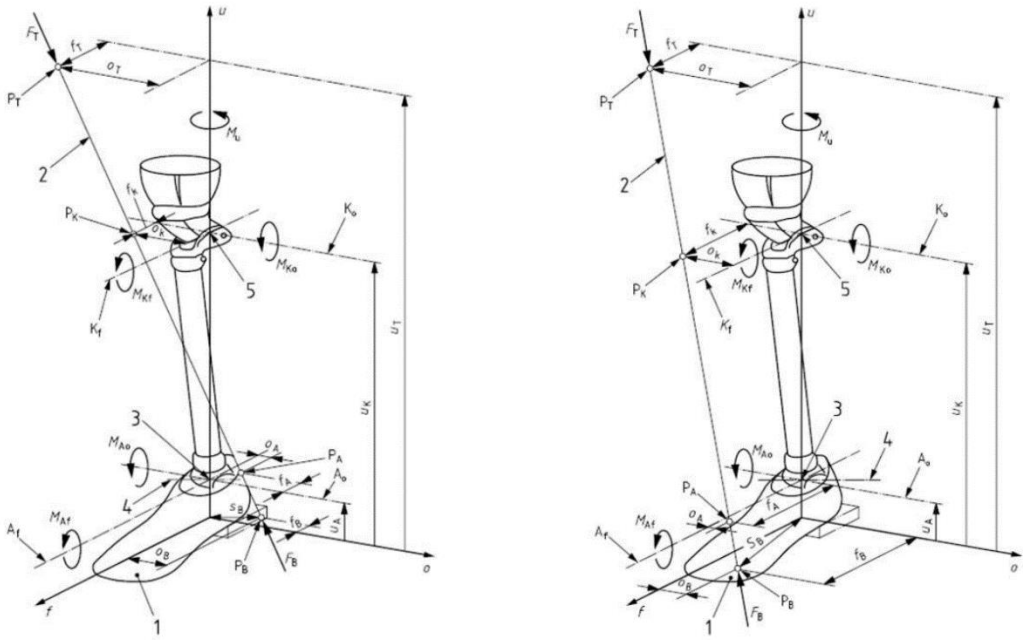

(a) *Configuration A* **(b)** *Configuration B*

Figure 2-6 (a) configuration a: maximum loading during heel strike (b) configuration b: maximum loading during toe off [24]

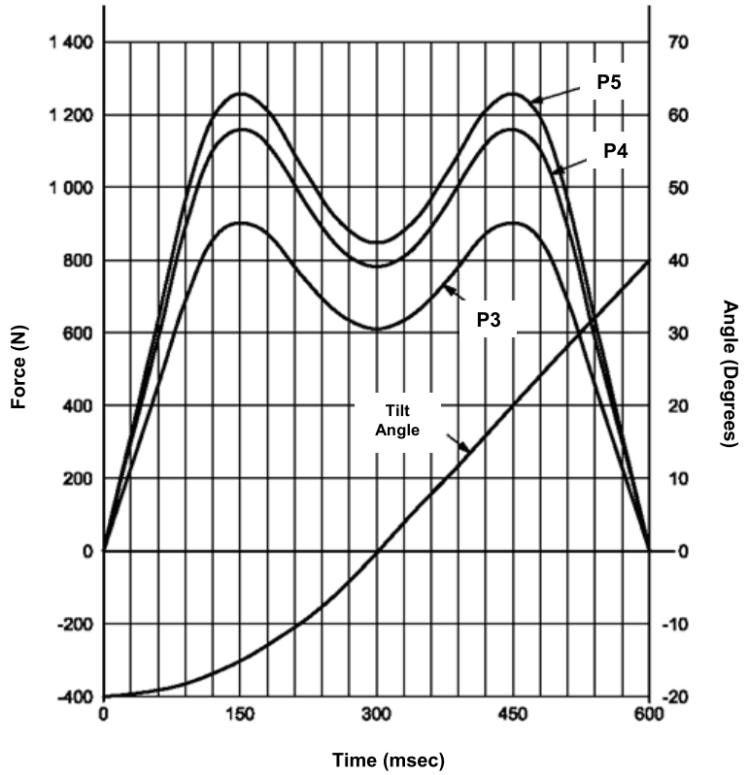

Figure 2-7 Vertical ground reaction force loading profile and tilt angle of foot against gait cycle as per ISO 22675-2016 [14]

Above mentioned conditions indicate the loading conditions and placement of test samples such that the critical load conditions are applied in true sense. The force applied to

the prosthesis is not aligned considering the fact of compound loading. Following tests should be performed to evaluate mechanical strength and endurance.

1. Proof strength test: Static load test applying 2000N force as shown in above two configurations to evaluate the maximum durable force of the prosthesis.
2. Ultimate Tensile: Ultimate tensile test provides maximum loading capacity of the prosthesis such that it is unusable.
3. Fatigue Test: Evaluating maximum loading capacity under cyclic loading.

ISO 10328:2016 elaborates test and monitoring criteria for sustainable load measurement and maximum displacement or elongation in the structure. The specimens under testing are approved against sustenance of load applied in accordance with the load curves generated using distinct weighted persons. It deals in static strength testing and cyclic testing of the specimen under consideration and acknowledges the limitations of standard regarding the performance testing of the system during its use. The standards state,

"Ideally, additional laboratory tests should be carried out to deal with function, wear and tear, new material developments, environmental influences and user activities as part of the evaluation procedure. There are no standards for such tests, so appropriate procedures will need to be determined." [27]

2.6 Lower Limb Prosthesis Testing

Lower limb prosthesis testing can be categories into following listed categories. These categories have certain pros and cons depending on the structure, assembly and control system developed for the prosthesis.

1- In vivo testing (Human-Based Testing)
2- In vitro testing / Hardware in loop testing

2.6.1 Human-based testing

Researchers and manufacturers use in-vivo testing criteria to understand the performance of prosthesis to overcome the limitations of ISO 10328:2016. In lieu of these, they have developed performance outcome measures that helps in predicting the functional characteristics and quality of living of amputee after using the prosthesis under consideration. These performance measuring indicators are developed using parameters such as oxygen consumptions, joint movements, moment, and forces generated while using the prosthesis and satisfaction level of patient using the prosthesis.

These performance measuring outcomes are segregated into three categories [20].

- Patient Reported Outcomes

- Performance Based Measures
- Biomechanical Measures

2.6.1.1 Patient-reported outcomes

These reports are generated on feedback of patient and assess constructs like satisfaction, quality of life and health functions.

- Amputee activity survey
- Prosthesis evaluation questionnaire (PEQ)
- Prosthetic profile of the Amputee
- Locomotor capabilities index
- Orthotic prosthetic users' survey (OPUS)
- Trinity amputation and prosthesis experience scales (TAPES)

2.6.1.2 Performance-based measures

The performance of patient is evaluated during task or group of tasks through performance-based measures.

- Amputee mobility predictor (AMP)
- Comprehensive high activity mobility predictor (CHAMP)
- Timed up and go test (TUG)
- Six-minute walk test (6 MWT)
- Southampton hand assessment procedure (SHAP)

2.6.1.3 Biomechanical outcome measures

The biomechanical outcome measures are divided into kinematic, kinetic, and temporal spatial parameters. It is not possible to measure all the parameters in a clinic setting. However due to recent advancements the selected biomechanical parameters can be measured with the help of specialized equipment.

- Symmetry in external work measure (SEW)

Although performance measuring outcomes enables the researchers to predict the quality of the prosthesis developed, it has numerous limitations that needs to be addressed. The limitations associated with in vivo test methods are listed below

- repeatability and reproducibility of results.

- poor safety level.
- lack of volunteers with a technical background.

These limitations tend to reduce the rate and quality of development and advancements in the field of prosthetics. Although work have been reported including development of fittings and supports for abled-bodied subject, its resulted in increase in percentage error for mimicking gait pattern and adoption of prosthesis by the amputees. It seems important to develop a robotic testing system that helps the researchers enhancing following parameters.

- Functional performance of modern prosthesis
- Provides comparison of developed prosthesis with ease
- Support advancements in prosthetics increasing repeatability and reproducibility
- Satisfy the increasing demand of fully functionable prosthesis becoming a part of assembly line

Common procedure for performance testing of a developed prostheses adopted in literature is human based testing. These procedures can broadly classify into two sub-categories:

1- Amputee test
2- Able bodied test using modified devices

The basic idea behind the development of prosthesis is to replace a missing anatomical structure. Hence, intuitively, the developed prosthesis is attached to an amputee and the kinematics and dynamics of gait pattern is compared with a healthy person. A knee ankle system comprising of active ankle and passive knee is assembled (CYBERLEG Alpha Prosthesis) and the system is tested on amputees and able-bodied patients [1]. Furthermore, robotic knee prosthesis is proposed at [28] using motor transmissions and control theories and the results are also compared using prostheses mounted on abled bodied. Similarly, [29] developed integrated powered ankle prosthesis working on electro-hydrostatic principles. During testing phase, the control strategy and ankle motion of the developed prosthesis was compared to abled bodied data.

The dynamic performance of the developed prosthesis is further evaluated using the dynamic parameters involved in human walking such as moment-torque (force – position) profile of lower limb [30][31][32][33], examination of mechanical energy level of active prosthesis [32][34], and the consumption rate of consumption of oxygen and carbon dioxide production leading to the calculation of metabolic rate of human during motion[33].

Previously, researchers had developed gait emulators that can be mounted on able-bodies and used to understand gait dynamic parameters during various motions of human body[35][36]. The major cause for the development of these emulators were due to lack of availability of amputee. The push of timing of ankle foot prostheses had a considerable impact on metabolic cost of push-of timing power [37]. The pneumatically actuated powered transfemoral device has been designed and tested using able-bodied testing adaptor for the evaluation of control systems and response of transfemoral prostheses prior to testing on amputee [38].

Figure2-8 Transfemoral Prosthesis Attached to Above knee amputee during step climbing test[39]

Figure 2-9 Walking Gait of prosthesis mounted on able-bodied using able-bodied testing adaptor [40]

2.6.2 In-vitro testing of Lower Limb Prosthesis

Researchers and Engineers performed cyclic testing of ankle prosthesis using Universal Testing Machine [14]. Moreover, they have developed mechanical structures for gait analysis and performance testing yet have been unable to use the simulator as cyclic testing of lower limb prosthesis. The gait simulators developed can be segregated into two types of systems: systems that track ground reaction force profile mentioned in ISO standards and interact with the foot accordingly and systems that generates gait profile of human walk [24].

The simulators and mechanisms fabricated for cyclic testing are mainly based on technologies involved in designing the mechanisms and control theories applied for the systems. These mechanisms are segregated mainly based on degree of freedoms provided to them in response to mimic the motion of hip, knee, or ankle joint i.e., considering movement in sagittal and transverse plane or just in sagittal plane. Most of the researchers considered motion in sagittal plane to introduce simplicity to the system. Moreover, the ground reaction force produced in these systems uses force plate mechanism or running platforms for actuation and measurement [24].

The simulators having the tendency to assess the functional capabilities of transtibial prosthesis are discussed in [41] and [42]. The former designed a test bench to study the ground reaction force using cadaveric specimens as test subjects. The test bench comprises of linear guide metallic framework for horizontal movement and force platform for ground reaction force. The foot specimen is hanged using hinge joint behaving as knee joint and the carriage and hinge are actuated through servo-electric motors making it 3 DOF system producing horizontal motion of prosthesis, rotation of hinge joint and ground force platform for vertical motion. The correct representation of test bench is shown in the fig 2-10(a). The study introduced inertial control for gait simulations that omit the use of predefined set points of vGRF during the gait simulations. The results obtained are observed to accurately reproduce physiological pattern of vGRF whereas the values among the test specimen varies significantly. The test bench proposed in [27] is for below knee prosthesis in single sagittal plane producing degree of freedom using hydraulic and pneumatic actuations as shown in fig 2-10(b). Vertical loads and movements are produced using hydraulic actuator installed at hip joint whereas horizontal motion of foot is produced using linear guide operated using electric servo motor. The rotation of thigh and knee joint portion during stance phase is produced using lockable gas spring. The passive control of joint rotations decreases the accuracy of kinematics and dynamics of test bench against the actual motion. However, introduction of lockable gas spring to hip hinge helps in attaching transfemoral prosthesis to the system. The active control provided using servo motors at [41] helps in accurate mimicking of dynamics and kinematic characteristics of the human gait pattern whereas additional hip rotation joint provided in [42]. provides the ability to attach transfemoral prostheses to the system with minor amendments in the system. However, both systems have limitations for providing platform for cyclic testing of the system due to the size of machine.

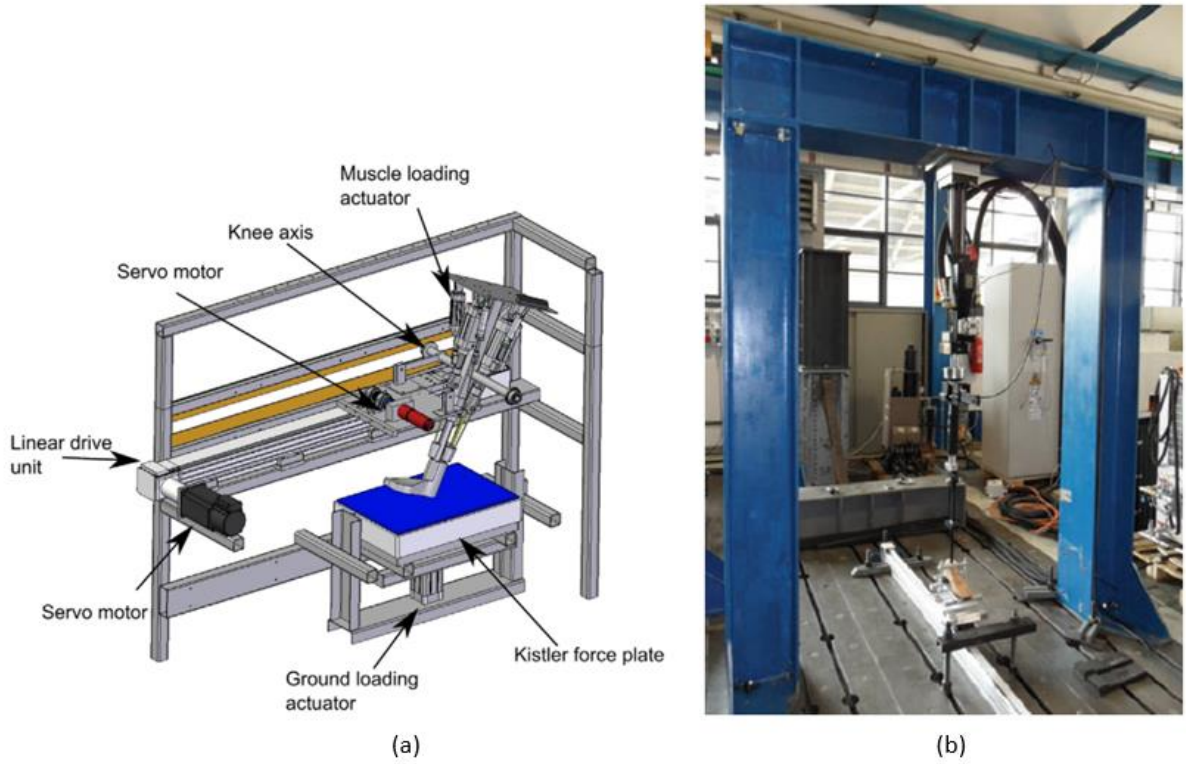

Figure 2-10 (a) Cadaveric gait simulator designed using a force plate to calculate ground reaction force exerted during a gait cycle [41] (b) Test bench designed to produce gait profile [42]

Similar architecture has been proposed by [43] having servo motor attached to hip joint controlling both hip and knee angular motion and running platform for generating continuous motion. Apparently, this architecture helps in reducing the constraints of cyclic testing and author claims the possibility to test transfemoral prosthesis, whereas there is no evidence for this opportunity. The fabricated test bench is shown in fig 2-11(c).

However, in [44], the researchers modelled and design two link semi-active transfemoral prosthesis using magnetorheological damper knee controlled through microprocessor. MR Damper installed in the knee prosthesis helps in controlling the torque dissipation by varying the current flow in solenoid. The electromagnet produced through the current flow changes the magnetic field around the solenoid that in return changes the MR fluid viscosity and damping value of the fluid. The designed prosthesis was tested using three DOF gait simulator abled to provide horizontal and vertical hip motion and rotational motion in sagittal plane as shown in fig 2-11(a) Knee joint tracking control was performed using the simulator through implementing repetitive controller along with PD control law and computed control law. This resulted in reduction of RMS error during swing phase whereas stance phase error is significant as ground reaction force is not tracked and controlled.

Figure 2-11 (a) 3-dof Gait simulator design using roller platform to perform cyclic gait profile [44] (b) 2-dof robotic test bench design using roller platform to perform cyclic gait profile [18] (c) bipedal leg prosthesis design [43]

The minimum requirement to produce gait motion in sagittal plane is three degrees of freedom including hip vertical and thigh rotational motion along with knee rotational motion[18]. To implement this concept, a test bench is fabricated to mimic the gait pattern. The vertical motion profile is implemented using ball screw mechanism whereas thigh rotation is performed using prosthesis directly coupled to 80:1 worm gearbox mounted on motor shaft as shown in fig 2-11(b). The vertical axis of the machine is fixed, and no movement is possible in horizontal axis of the system. Hence, treadmill is used to provide cyclic motion to the system. This setup opens the possibilities to assess the prosthesis under consideration during different loading conditions. The dynamic model of the system is developed and sliding mode control scheme is implemented to assess the torque profile required to produce vertical and rotational gait positions of human leg. The required current and voltage profiles of the system are calculated and compared to modelled and desired values.

On the contrary, *department of mechanical engineering TU Berlin* developed a 5-axis servo-hydraulic actuator controlled lower limb prosthesis test bench as shown in fig 2-12(a) [45]. Three actuators represent the hip movement of flexion/extension, adduction/abduction, and eversion/inversion movements whereas the remaining two actuators represents the horizontal and vertical movement of force plate mechanism generating necessary ground reaction force. A microprocessor-controlled knee prosthesis along with passive prosthetic foot is attached to the system. Each actuator is attached to strain gauges to gather moment data and an additional six DOF force and moment sensor is installed within the prosthetic knee for reference of simulator control. The obtained results are good for stance phase

whereas movement and load data of hip and knee joint during swing phase deviates from the gait analysis data; this deviation in data is due to the inaccurate inertial load distribution after constraining displacements linearly. Consequently, the data gather from rotation of thigh and shank deviates from gait analysis data.

Most of the researchers reduced the degrees of freedom of gait simulators to increase controllability and provide ease to the system. However, this also neglect the impact of motion of hip in frontal and horizontal plane. The researcher in [24] attempted to produce gait pattern of hip joint in accordance with the effect of ground reaction force by using hydraulic manipulator for generating horizontal and vertical ground reaction force and industrial robot for hip translational and rotational motion as illustrated in fig 2-12(b). Despite using industrial 3dof robot to mimic hip translational and rotational motion, gait pattern deviations have been observed in longitudinal direction. The author suggested the cause of deviations to the contact of force plate to the prothesis. Moreover, using an industrial robot increases the cost of the system which has a negative impact in developing countries.

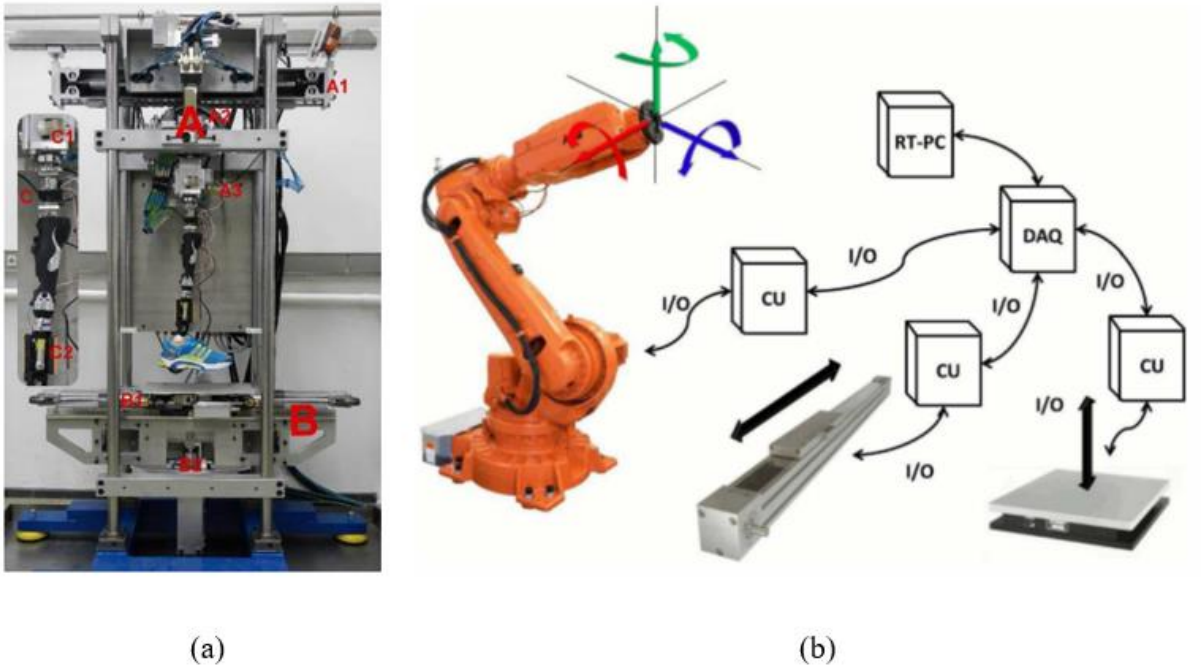

(a) (b)

Figure 2-12 (a) 5-dof hydraulic actuator operated gait simulator for testing transfemoral gait prosthesis [45] (b) 8-axis gait simulator mechanism including 6-dof industrial robot for hip translational and rotational motion and 2-dof base plate platform for generating vGRF [24].

CHAPTER 3: DESIGN AND FABRICATION OF TEST BENCH

A 2-DOF Robotic platform for testing transfemoral prosthesis is designed and fabricated that can perform cyclic testing of transfemoral as well as transtibial prosthesis. The methodology adopted to design and fabricate testbench is shown in figure 3-1.

3.1 Conceptual Design:

The minimum requirement to mimic a gait cycle is to reproduce hip vertical and thigh rotational motion in sagittal plane. The motion profiles of hip joint, knee joint and ankle joints are important parameters and prerequisites to understand the torque, power, and energy requirements. The elaborated gait data is taken from literature and hip vertical motion profile and thigh rotational motion profile is extracted from the dataset [46]. The Dataset is compiled using 12 abled bodied subjects and comprises of 12 files illustrating the kinematics and kinetics of human walk. The first file consists of description of model developed to extract human gait profiles. However, the motion profile data of the ankle, knee and hip profiles are listed in "kinematics.xls" file and are extracted for simulating the mechanism.

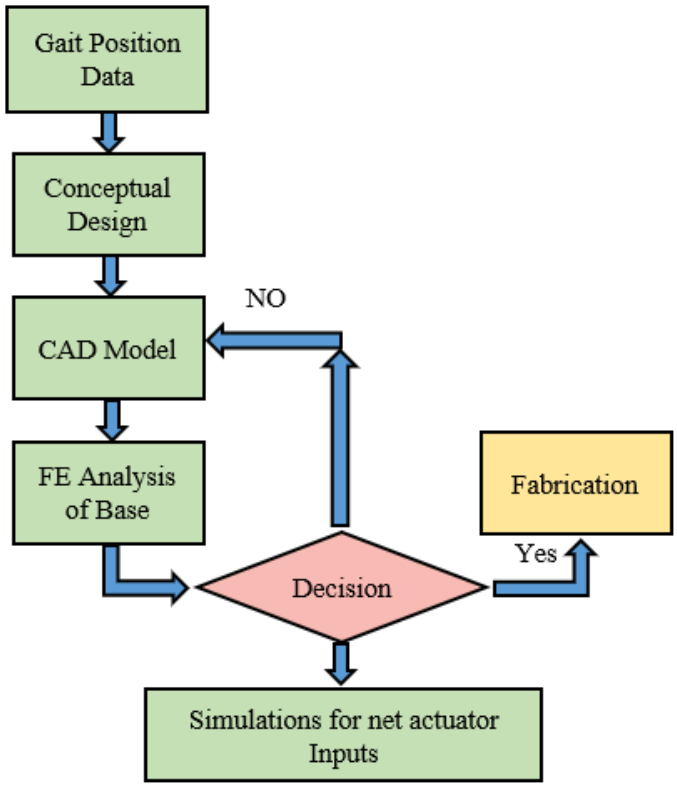

Figure 3-1 Methodology adopted for design and fabrication of test bench for transfemoral prosthesis

Table 3-1 Design Criteria for Linear carriage system and Rotary drive system

Sr#	Parameters	Dimensions	Design Values
Mechanism for hip vertical			
1	Hip displacement	Δy_{hip}	50 mm
2	Hip angles	$\Delta\theta_{hip}$	50 deg
3	Maximum force	$F_{y,\,hip}$	1200 N
4	Maximum speed of carriage	$v_{y,\,hip}$	1 m/s
Hip Rotational Motion			
5	Maximum torque	$M_{z,\,hip}$	75Nm
6	RMS speed	$w_{z,\,hip}$	150 deg/s

The machine is divided into three sections: A vertical carriage system, rotational block system and treadmill as running platform. The design criteria for vertical carriage and thigh rotational system is extracted from the gait dataset in accordance with the benchmark paper and is listed in the table 3-1 [18].

3.2 CAD Models

A computer aided design (CAD) model is generated in Solidworks® to visualize process of the system and assists in fabrication. The model illustrates the mechanical assembly of test platform including the vertical carriage motor mounting assembly, ball screw, the vertical carriage, rotational motion mounting assembly, circular disk holding a transfemoral prosthesis.

The developed model is used for the fabrication of test bench rectangular base and assemblies. Moreover, the assembly is exported to MATLAB Sim-mechanics® for simulating torques and velocities required for the hip vertical and rotational motion. It is noted that the knee and ankle joint is considered as a pin joint to simulate the walk pattern. The design is revised numerous times to produce a layered model of Simscape multibody® corresponding to the actual design and to align the rigid transform blocks of Simscape® for providing rotational motion. The CAD model of test bench is shown in figure 3-2.

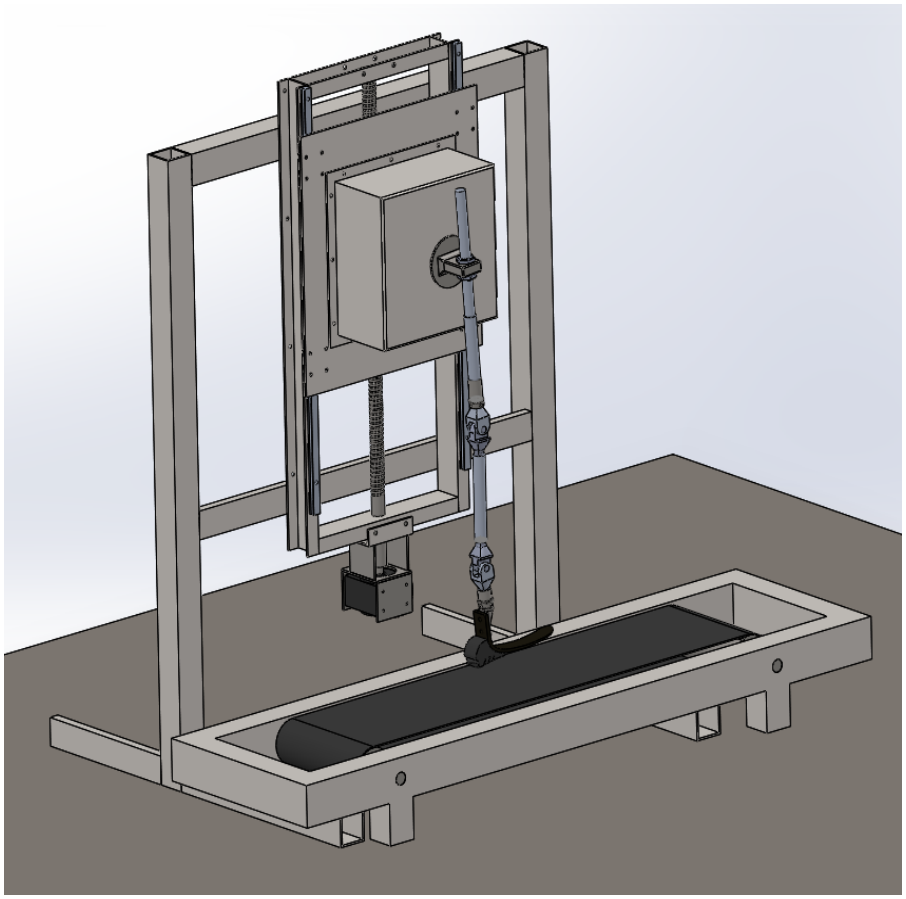

Figure 3-2 CAD Model of Test Bench

3.3 Detail Design of Test Bench

3.3.1 Vertical Drive Mechanism

The vertical carriage comprises of a ball screw mechanism coupled to a 5:1 worm reducer which in return is coupled to a 19mm motor shaft. The motor gearbox housing is bolted to the base frame of the test bench to provide support to the motor. The carriage of ball screw is mounted to U shape iron holder welded to 400mm x 600mm x 5mm metal plate. The metal plate is bolted to square box encapsulating motor-2 for rotational motion. A circular disk welded to a square is fabricated having 25mm hole to mount the shank of prosthesis. The parameters for designing and selecting the vertical motor and drive are listed in table 3-2. According to the design criteria listed in table 3-1, the vertical actuator is designed to lift a mass of approximately 122.3 kg for a linear velocity of 1 m/s. This corresponds to the requirement of generating maximum vertical ground reaction force of 1200N as mentioned in ISO standard and corresponding loading profile represented in figure 2-7.

The Linear carriage motor torque requirement according to the given data is calculated to be 1.5617 Nm. The required torque is calculated using the motor calculation procedure listed in motor brochure and attached as appendix A. Moreover, code for calculating maximum torque value is listed as appendix B.

3.3.2 Rotational Drive Mechanism

The rotational drive is calculated in accordance with the values of torques and rotational motion listed in design criteria mentioned in table 3-1. The design value of rotational torque and angular velocity is 75Nm and 150deg/s respectively. The motor selected for hip rotational motion has rated torque value 1.3Nm. The shaft of rotational motor (motor2) is coupled to 80:1 gearbox to generate designed torque and rotational speed.

3.3.3 Motor specifications and power circuit

A 750 Watts Mitsubishi (HF-KP73) motor (motor1) with Mitsubishi amplifier MR-J3-70A (driver1) is selected for powering vertical carriage and Mitsubishi HF-KP43 motor (motor2) with MR-J3-43A amplifier is used to generate designed torque and rotational speed for hip rotational motion.

Ac servo motor operates at both three-phase and single-phase power supply. The requirements for powering up the servo motor and drives are listed in the manual. The power requirement of motor1 and motor2 selected for the operation are 750watts and 450watts, respectively. The maximum current that the winding of motor1 can bear at 350% of torque is 15.6 amps without damaging the windings of the motor. However, the continuous torque of vertical drive is 2.4Nm at continuous speed of 3000rpm. Similarly, maximum current of motor2 that motor can withstand at 350% of torque is 8.1amps without damaging the windings of the motor. However, the continuous torque is 1.3 Nm at continuous speed of 3000rpm. These parameters values are extracted from the specification table in the manuals of respective motors and are attached as appendix C.

Table 3-2 List of parameters for selection of linear and rotary servo motors

Sr No	Parameter	Units	Measurement	Description
	Vertical Mechanism Parameters			
1	Total Mass	Kg	120	Total mass of driven system
2	Max linear speed	m/s	1	Linear speed of carriage
3	Alpha angle	Deg (°)	90	Ball screw tilt angle
4	Ball Screw length	mm	1	Ball Screw Length
5	Guide Travel	mm	300	total span of travel
6	Ball Screw Diameter	mm	32	Ball Screw Diameter
7	Ball Screw lead	mm	10	Ball Screw pitch/lead
8	Ball Screw Efficiency	%	80	Ball Screw efficiency
9	Ball Screw density	Kg/m^3	7500	Ball Screw Density
10	Internal friction of preloaded nut, μ_0	n/a	0.2	Internal friction coefficient of preloaded nut.
11	Coefficient of kinetic friction, μ	n/a	0.05	Friction coefficient of sliding surface
12	Safety Factor	n/a	2	
13	Gearbox Efficiency	%	0.86	
	Rotational Parameters			
14	Angular velocity	°/s	150	Angular velocity of the thigh
15	Torque	Nm	75	Thigh Angular Torque

Mitsubishi servo motor can provide position, speed and torque control for a system. It can also shift control modes during real time processing; it can shift position control to speed control or speed to torque control or torque to position control or vice versa. A start-up logic

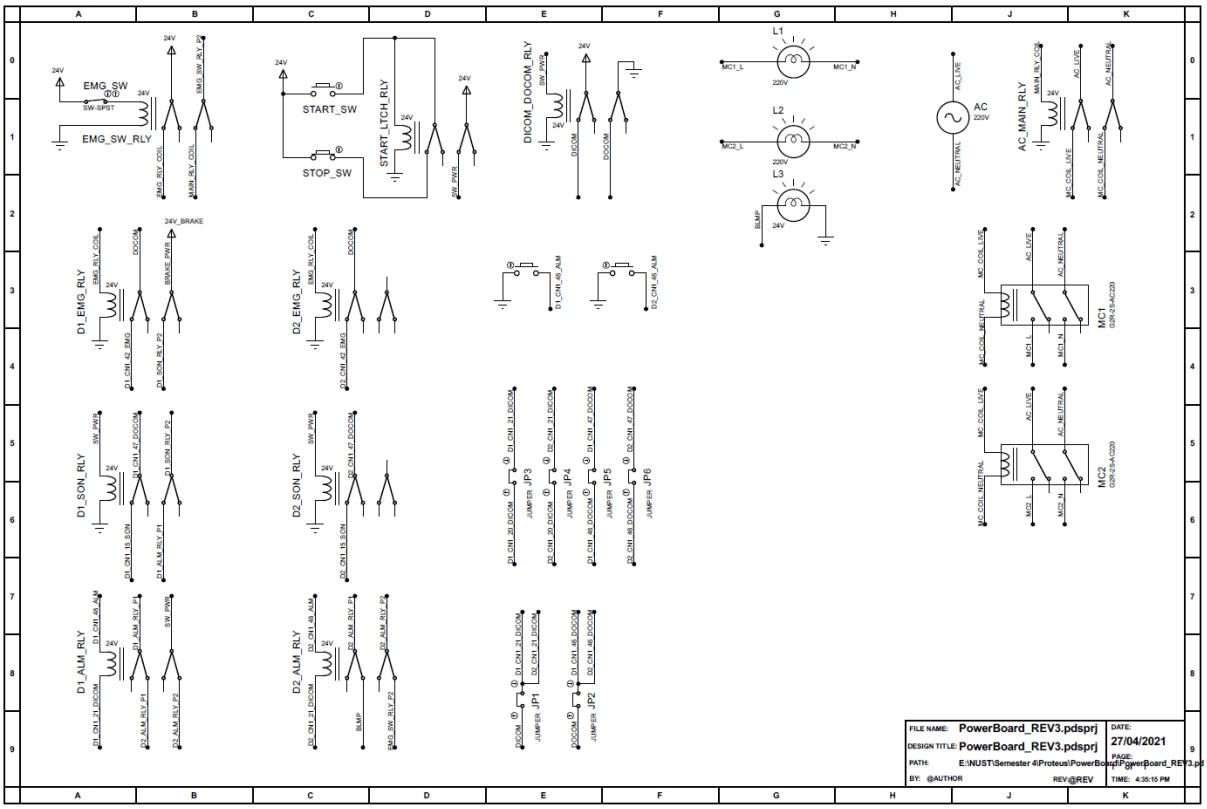

Figure 3-3 Power board logic design

is required for the smooth operation of servo drives including system halt at alarm raising and providing emergency stop to the system. The control inputs associated to starting of servo motor are servo on pin (SON), reset pin (RES), Limit Switch pins (LSP, LSN), Alarm Status (ALM) and a latching circuit for power buttons.

Accordingly, a start-up logic is developed in proteus8.0® simulator to energize servo motors and drives and at the same instance, it halts the system power in case of alarm generation or when emergency is pressed. The logic circuit is developed considering input-output connection diagram for position control mode listed in servo drive manual (MR-J3 - A). The I/O connection drawing associated with the power-up logic is attached as appendix D. According to the manual, the start-up logic for all control modes is same. However, I/O connections increases for implementing control logic. Hence, the logic caters the least requirement for operating servo motor in position control. The generated logic is physically implemented using layout plan drawn in autoCAD®. The drawings associated with the logic development is shown in figure and layout plan is attached as appendix E.

3.4 Simulation of Human Gait Profile

The finalized CAD model design of test bench was exported to MATLAB sim-mechanics® for simulating the gait profile by providing the four input profiles: Hip vertical

displacements, thigh angular displacements, knee angular displacement and foot angular displacement. Figure 3.3 shows the profiles of hip, knee and thigh were extracted from dataset in the literature [46]. The values of Right foot profile are taken for simulating the gait pattern.

Firstly, Solidworks® extension file is installed and registered in Matlab® software. The design file of Solidworks® is then export to sim-mechanics® extension modules created in Solidworks® in the results of both software integration. The step files of CAD design are created by Solidworks® and an .xml is created describing the material properties and joint configuration of design under consideration. Furthermore, .xml file is read in the MATLAB Simscape® to generate a Simscapes® model of the system. The generated Simscape multibody® model is attached as appendix F. Revolute joints have been introduced at ankle, knee and hip pins whereas as for hip vertical motion a ball screw joint is modelled using lead screw modules. The dataset is imported in MATLAB and right hip data is extracted from the dataset and passed to the module using Repeating Sequence Interpolation block. The joint block introduced in the model are provided with linear and angular displacements and corresponding angular velocities, angular accelerations and torque values required for desired motion. The curves of net actuator inputs required for hip vertical motion and thigh rotational motion are shown in figure 3-4. It is noted that these profiles show torque profiles for swing motion.

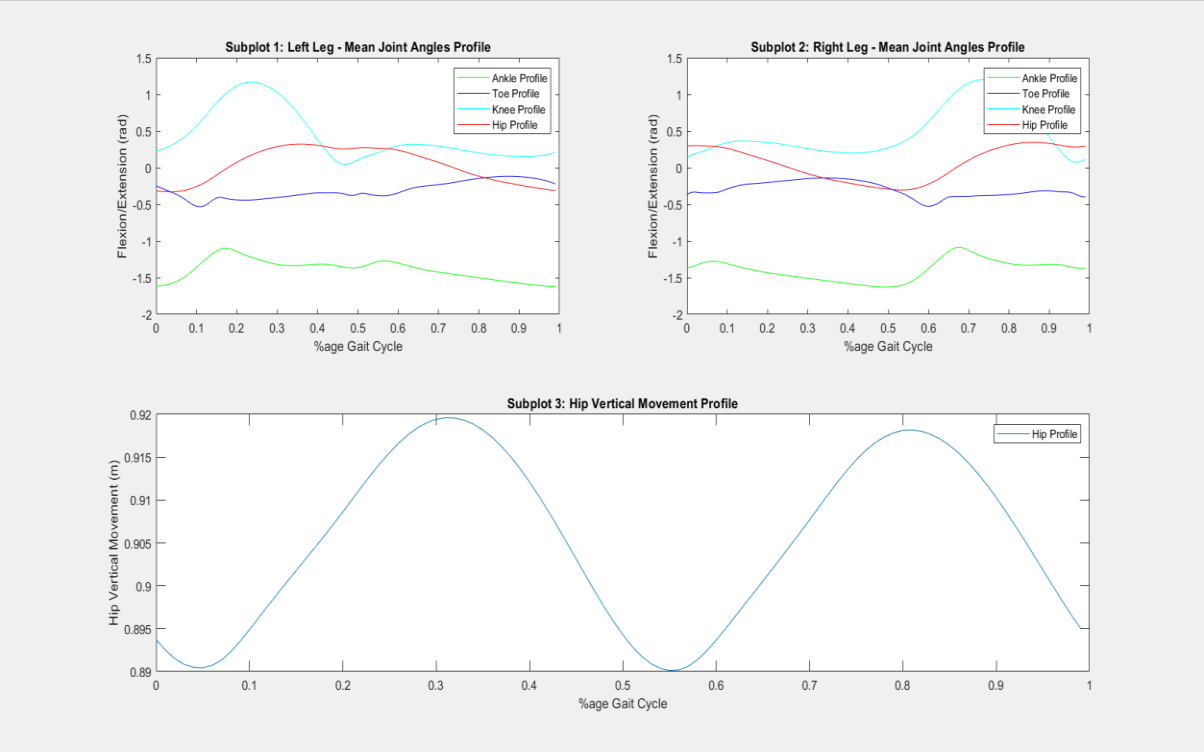

Figure 3-4 Hip, knee and foot linear and rotational profiles used for test bench simulations

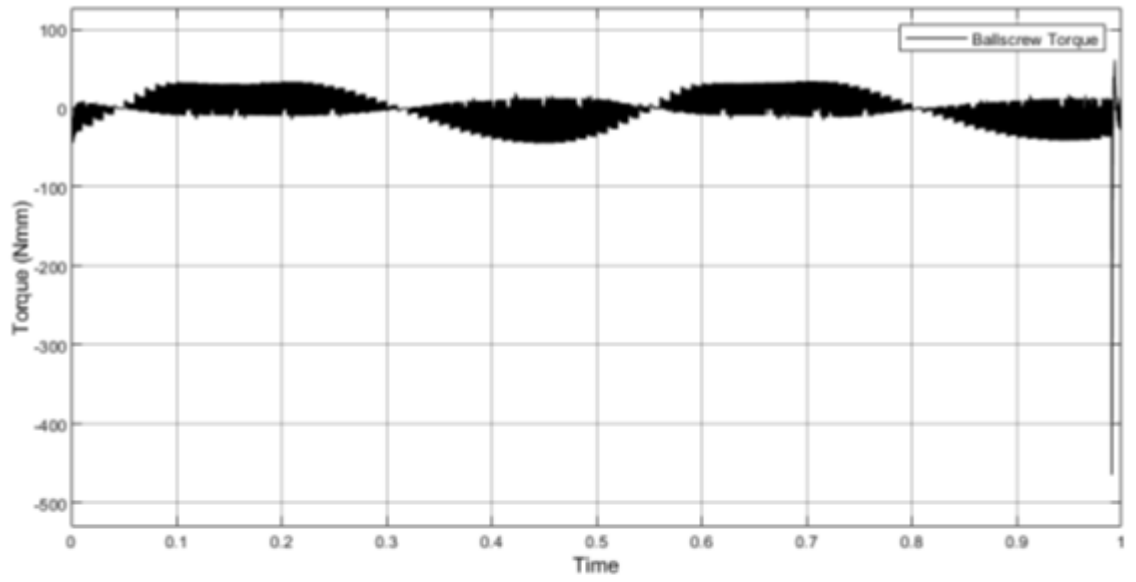

(a)

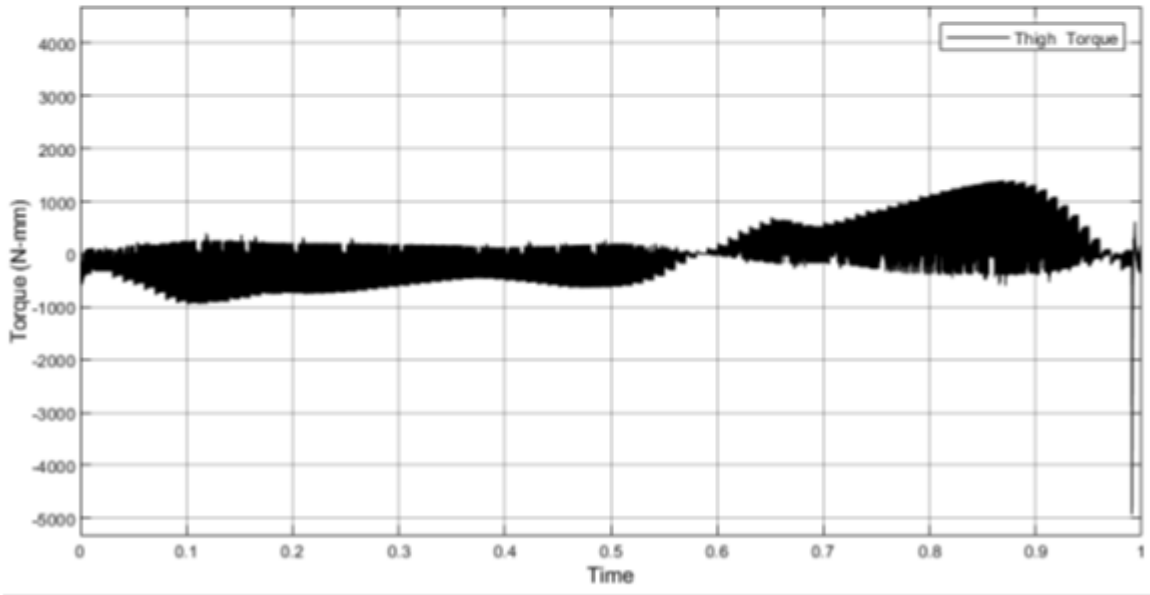

(b)

Figure 3-5 (a) Net actuator inputs required for hip vertical motion (b) Net actuator inputs required for thigh rotational motion

This net actuator torques are verified by passing gait profile data to Euler-Lagrange equation for PRR robot equation extracted from the literature[18]. The equation is listed as follow.

$$D(q)\ddot{q} + C(q,\dot{q})\dot{q} + J_e^T F_e + g(q) = F_a$$

Where:

q = joint angular position

q(dot) = joint angular velocity

q(d.dot) = joint angular acceleration

D(q) = Inertia Matrix

C(q,qdot) = Centripetal and Coriolis Matrix

J_e = Effective Jacobian at the point of application of Force

F_e = Impact force vector between foot and belt

g(q) = Gravity Vector

When the impact is not considered, the equation reduces to

$$D(q)\ddot{q} + C(q,\dot{q})\dot{q} + g(q) = \tau$$

Where τ is net actuator inputs for the system.

3.5 Fabrication of test bench

3.5.1 Fabrication of Mechanical Structure

The base and drive mechanism of 2 DOF robotic platform is fabricated in National Center of Robotics and Automation (NCRA) in Robot Maker Lab (RML) and is shown in figure 3-5. A structural steel 75mm square duct is used for fabricating the base platform of the structure. The base structure is welded with the 75mm x 25mm U channel duct for the housing the ball screw of vertical drive mechanism. The ball screw is coupled to worm gear reducer hub shaft using a mild steel coupling and the motor shaft is coupled the worm shaft. A 5:1 worm gear reducer is used to cater the inertial torque requirement of the mechanism.

Figure 3-6 Fabricated Mechanical Structure for transfemoral prosthesis

Motor generating hip rotational motion is coupled to 80:1 worm gear reducer to increase the motor torque as per design specifications mentioned in table 3-1. The gearbox in return is mounted in 400mm x 400mm x 200mm square hollow box using bearing and M4 screws as shown in CAD model in figure 3-2. The Hollow box is fixed with the 600mm x 650mm x 5mm metallic sheet which moving as linear carriage using ball screw carriage using a 20 mm thick metallic sheet having U channel within it. This implies that the whole weight of the rotational mechanism and metallic box holding sheet is driven by the ball screw carriage which is operated by 750 watts vertical motor and amplifier. To couple

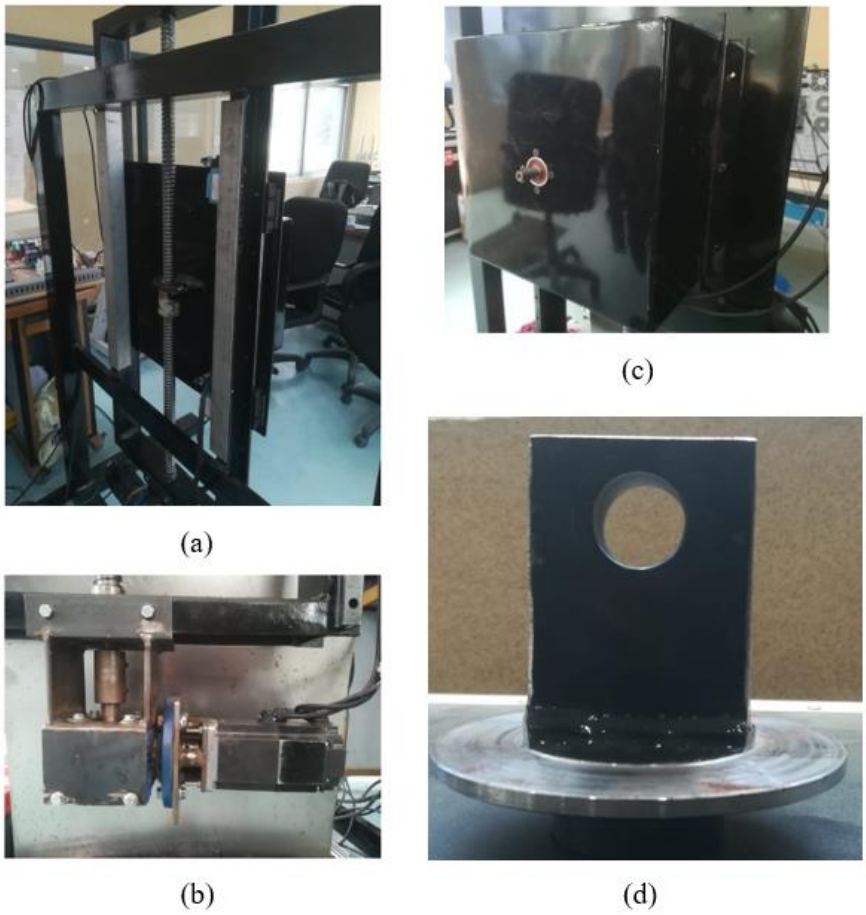

Figure 3-7 (a) Vertical drive assembly (b) Vertical drive motor coupling and mounting assembly (c) Rotational drive motor position (d) Fabricated Circular disk

transfemoral prosthesis with the hip rotational motor (motor2) a fabricated part comprising of circular sheet welded to a 20mm thick iron square piece as shown in the figure 3-6(d).

3.5.2 Assembling of Transfemoral Prosthesis

The transfemoral prosthesis assembly consist of a passive foot and knee prosthesis screwed to adapter tube assembly extensively used for transfemoral and transtibial prosthesis development. The length of pylons are adjusted using height distribution mentioned in literature as shown in the figure 3-6(a) [47]. The length of lower shank and upper shank are adjusted to 0.485m and 0.417m respectively which corresponds to the average height of 1.7m of Pakistani people. The length of the lower shank is fixed however the length of the upper shank can be adjusted using 300mm long screw press fitted to the upper shank. It can help vary hip height according to the prosthesis under study. The upper shank is bolted to the fabricated part mentioned in section 3.4.1, having a 25mm hole, to adjustable screw using the 25mm thick nuts. The assembly of transfemoral prosthesis used is show in figure 3-6(b).

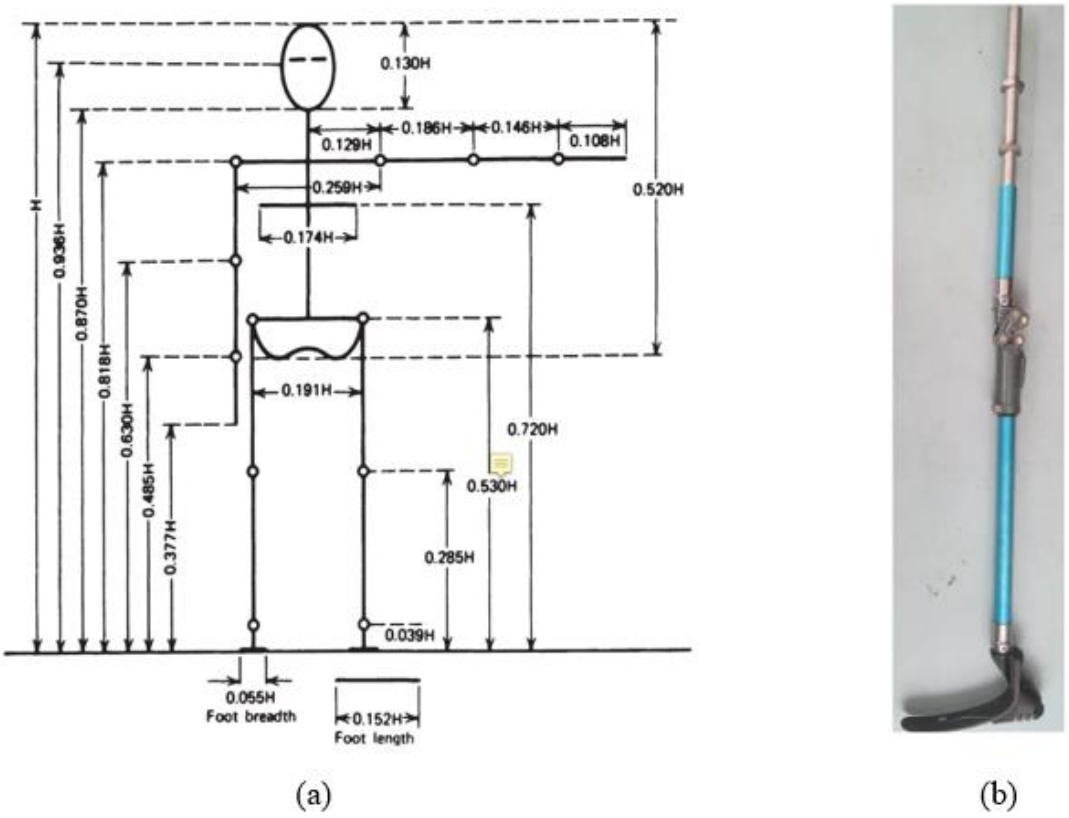

Figure 3-8 (a) Aspect ratio of lower limb to human body [47] (b) Lower limb prosthesis developed for Test Bench

3.5.3 Fabrication of Power Distribution Board

The power distribution board was fabricated using layout plan generated according to start-up logic developed. The Bill of material for power distribution board is listed in table 3-3. The component used are recommended in the manual to drive the servo motor. The fabricated power board is shown in figure 3-8.

Noise reduction techniques are applied to the system at power level and control level to reduce the noise associated with the power lines and frequency drives. These techniques include

1. Coiling of 220V line wire around toroid to reduce electromagnetic effect AC line on drive signal cable.
2. Installing radio noise filter and line noise filter on main AC line.
3. Installing surge absorbers between line and neutral of contactor.
4. Earthing of metallic structure.
5. Placing control circuitry in metallic casing which is properly earthed.

Table 3-3 Bill of Material for Power Distribution Board

Sr#	Item Description	Units	Quantity
1	30 Amps Circuit breaker	Nos.	2
2	12 Amps Magnetic Contactor	Nos.	2
3	24V DC Relays	Nos.	8
4	24V Power supply	Nos.	2
5	5V Power supply	Nos.	1
6	Terminal strips	Nos.	3
7	Momentary Push Button Red	Nos.	1
8	Momentary Push Button Green	Nos.	1
9	Emergency Stop	Nos.	1
10	Reset Switch	Nos.	1
11	Cable Duct	m	3.66
12	Perforated Strip	m	2

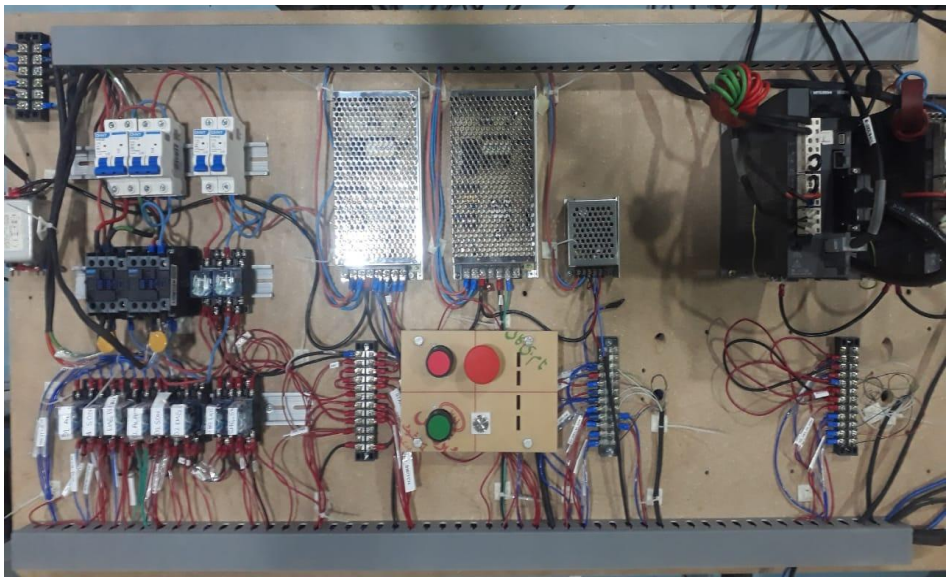

Figure 3-9 Fabricated Power Distribution board

CHAPTER 4: CYCLIC TESTING USING FEA TECHNIQUE

It is pertinent to perform mechanical and functional testing of prosthesis before providing it to the end user. As mentioned in literature, the mechanical testing of lower limb prosthesis is performed according to ISO 10328:2016 and ISO 22675:2016 [14]. However, for functional testing, the standard provides leverage to develop a setup that may provide an environment to perform gait analysis of prosthetic foot using in-vivo or in-vitro testing procedures[24]. ISO 10328:2016 narrates four sequential tests, listed as below, that helps in understanding the mechanical behavior of lower limb prosthesis under study.

1- Initial static-proof test
2- Ultimate tensile strength test
3- Cyclic durability test
4- Final static proof test

Among the above-mentioned tests, cyclic durability testing is crucial that helps in understanding the behavior of prosthesis during usage. The standard provides an M-shape curve of vertical ground reaction force (vGRF) and tilt angle of foot prosthesis as a function of stance phase time, as shown in figure 2.7. The curve depicts testing profile for stance phase of gait cycle. The time axis shows 600ms for stance phase of gait cycle having period of 1 sec. Three separate curves show the load bearing capacity of prosthesis tested according to their respective profiles. P1, P2 and P3 profiles corresponds to 60kg, 80kg and 100kg load bearing capacity of prosthesis at study. As per standard, foot prosthesis having the ability to withstand loading profile will have life of 300,000 cycles comparative to 3 years of normal use. Researchers have performed cyclic testing using material testing machine by adjusting pylon and applying force at heel and toe region[20]. The methodology adopted is also implemented using FEA tools to reduce the setup cost and provide a simulation base platform for cyclic testing[48].

Finite element method technique (FEM) provides a room to perform mechanical strength tests in simulation reducing the cost of production of equipment or product in consideration. These methods have been rapidly used by engineers to develop both upper and lower limb prosthesis and their sockets[49]. The study involves design and development of energy storage and return (ESAR) foot involving having the ability to store energy during heel strike and mid stance phase of gait cycle and releasing it during that toe assisting the amputee in propulsion phase[15].

4.1 Methodology:

The purpose of performing the analysis is to conduct FEA based simulations at heel and toe region of prosthetic foot inspired by Sierra foot® to analyse the durability of foot in study. The methodology of study adopted is similar to methodology in literature at [48] and is shown in figure 4-1. Fifteen critical points have been gathered from the literature that scientists have already used for testing different types of prosthesis including Sach®, Niagara®, Axtion® etc. The foot prosthesis is loaded under critical points at prescribed angle and the maximum deformation values have been recorded. The deflection of heel and toe regions have been observed and stiffness values are calculated.

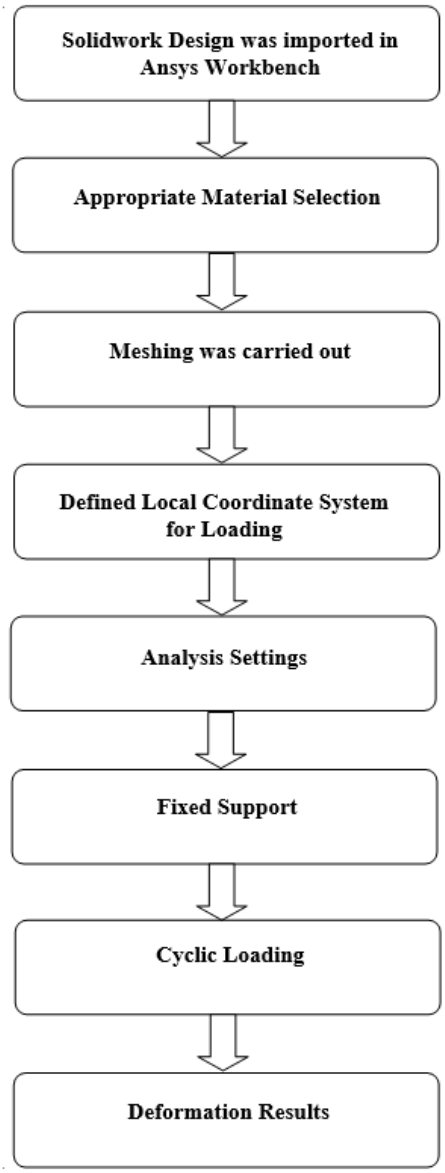

Figure 4-1 Methodology adopted for cyclic testing using FEM [20], [48]

4.2 Critical Points

As discussed earlier, critical data points from P4 curve of ISO waveform are extracted representing the force and time against angle of foot prosthesis. The values of force and time are recorded at angles with the increment of 5° for both heel and toe region and listed in table 4-1.

Table 4-1 Critical data points extracted from ISO 22675 [20], [48]

Section	Point	Time (msec)	Angle (°)	Load direction	Load (N)
Heel Region	1	0	-20	Loading	0
	2	36	-19.5	Loading	354
	3	150	-15	Loading	1173
	4	212	10	Unloading	983
	5	260	-5	Unloading	821
	6	300	0	Unloading	785
Toe Region	7	300	0	Loading	785
	8	337	5	Loading	831
	9	372	10	Loading	885
	10	408	15	Loading	1100
	11	450	20	Loading	1173
	12	487	25	Unloading	1062
	13	522	30	Unloading	769
	14	560	35	Unloading	392
	15	600	40	Unloading	0

A force against stance time and angle curve is drawn from critical points and shown in figure 4-2. The curve indicates 0ms for heel strike point (initial point). This constraint bounds the curve to 0N applied force. To overcome the constraint of starting value, the data point is taken at -19.5° form the graph and record for simulation purpose. It is noted that positive angle indicates plantar flexion whereas negative angles indicate dorsiflexion. Figure indicates the P4-level curve for stance phase generated from critical data points [20].

.

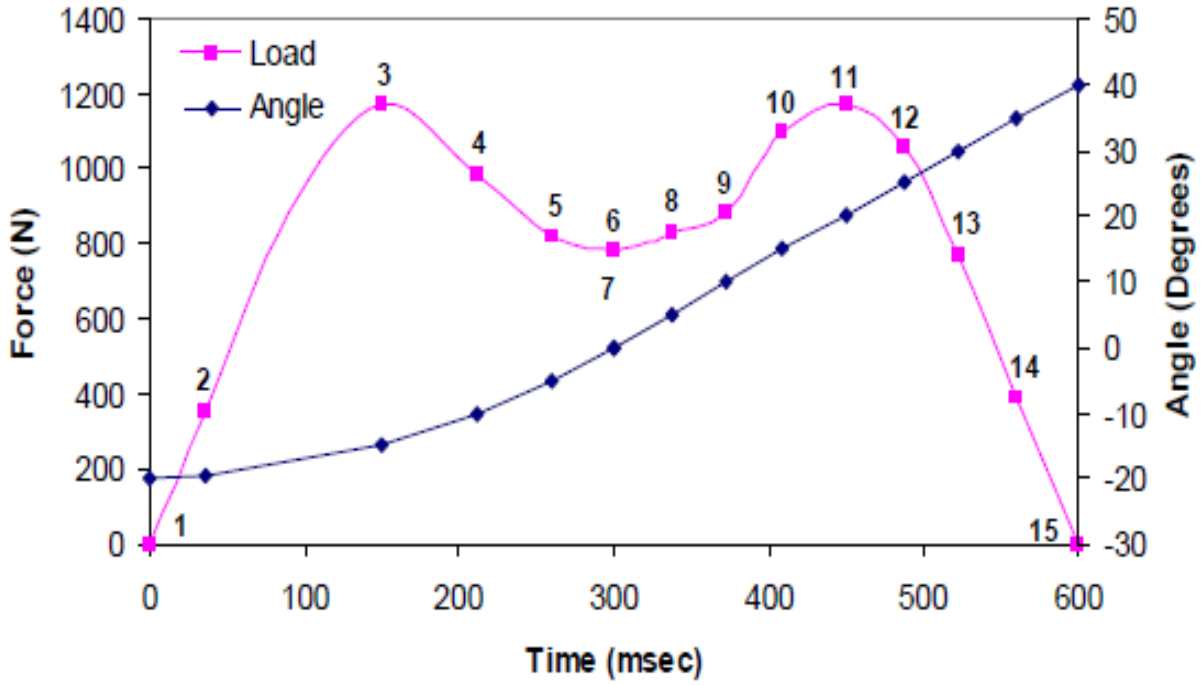

Figure 4-2 Cyclic durability curve generated by critical data points [20], [48]

4.3 Analysis Metrics

As discussed, ESAR foot stores energy during heel strike and mid stance and releases it during toe off, through stiffness of the material. The analysis metrics considered in the literature is shown in table 4-2.

Table 4-2 Analysis metrics considering ESAR foot prosthesis extracted from research on Niagara Foot™ [15][40]

Parameters	**Value**
Maximum value of deformation in heel region	8 mm
Maximum value of stiffness in heel region	680 kN/m
Minimum value of deformation in Toe region	40 mm
Maximum value of stiffness in Toe Region	280 kN/m

4.4 FEA Analysis on foot prosthesis

A CAD Model of foot prosthesis based on Sierra® foot prosthesis is designed in Solidworks® and imported in Ansys® for mechanical strength tests. The model is imported to Ansys Workbench® for calculating the total deformation at heel and toe region after the application of force at specified angles. The regions for application of force are created in the model through split face command and critical point forces are applied to the respective regions considering application of force in heel and toe region as stated in table 4.1. The critical point vGRF is resolved in x- and y- components to apply force at required stated angles. Two test are necessary to understand mechanical strength and endurance of foot prosthesis: proof strength test and cyclic durability test [48].

The meshing enhancement criteria is applied to increase the quality of tetrahedrons in ultimately increasing the quality of mesh and results obtained for maximum deformation. The figure 4-3 (a), figure 4-3(b), figure 4-3(c) shows the quality graph of mesh indicating the distortion in elements of mesh created. The colour contour represents the quality of mesh elements, tetrahedrons in this case, created for prosthesis. However, the distribution of mesh elements in the contour relative to quality of element is illustrated using bar graph shown in figure 4-4.

As per ISO standard, proof strength test is performed on designed model wherein a 2000N force is applied on heel region at -15-degree position of the foot with the ground. Same force is applied in toe-region at 20-degrees for maximum deflection and stress analysis. It is observed that the maximum stress generated in heel region is 1099 MPa with maximum deformation of 7.9606 mm. Similarly, maximum stress generated in toe-region by application of force at 20 degrees is 3544.44 MPa and the maximum deflection in toe-region against applied force is 31.151 mm. The values of maximum stress and maximum deflections are less than the values mentioned in analysis metrics indicating validating the strength of design in mechanical proof test. Figure 4-5 and figure 4-6 illustrates the maximum stress and maximum deflection in heel and toe regions respectively.

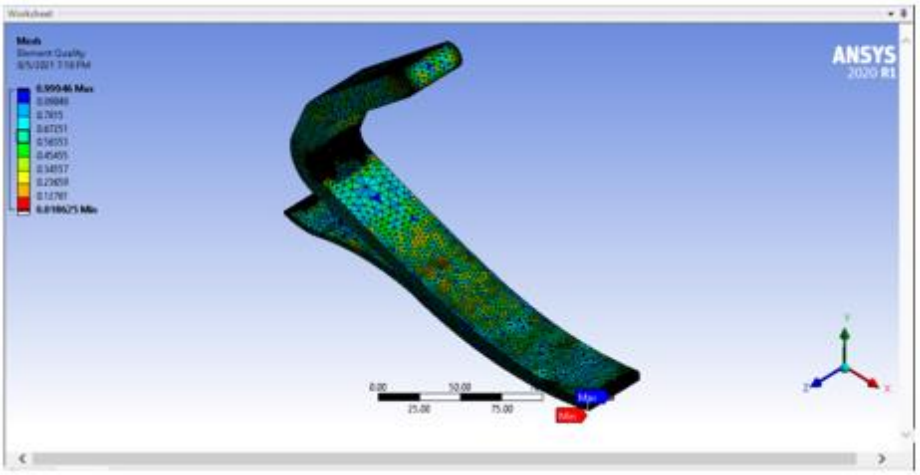

(a)

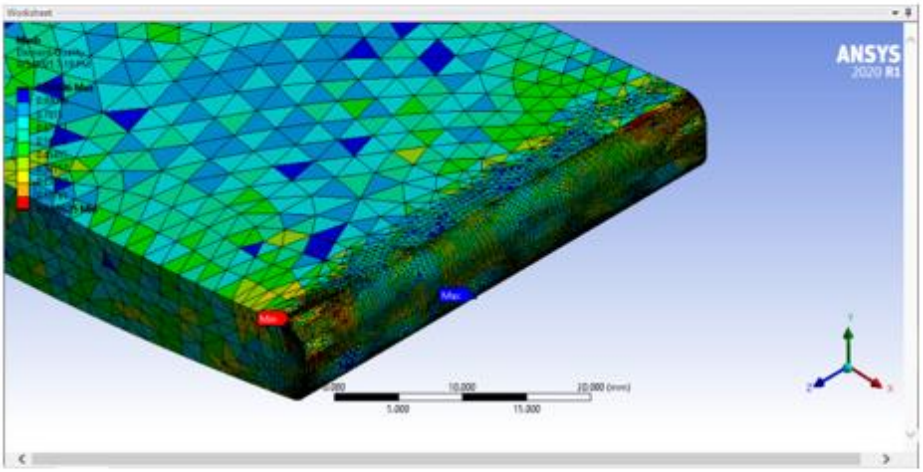

(b)

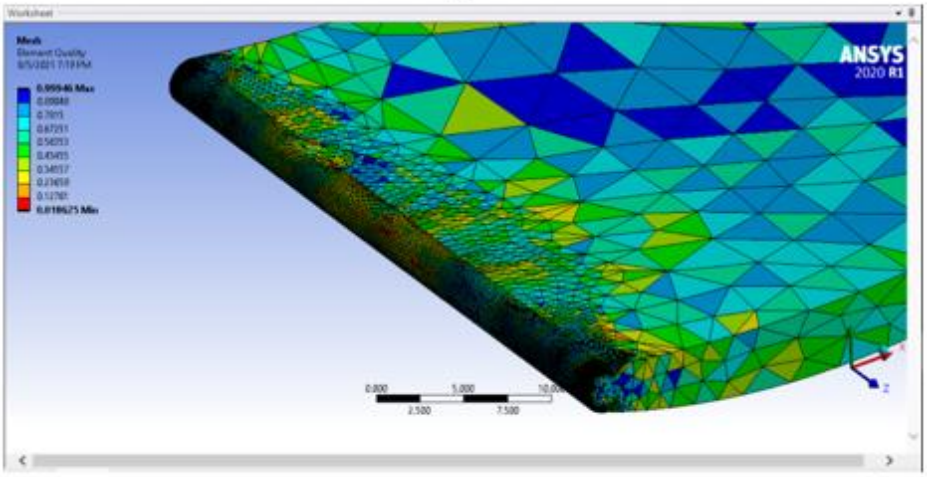

(c)

Figure 4-3 Meshing details of foot prosthesis (a) Quality of mesh in foot prosthesis (b) Quality of mesh in toe region (c) quality of mesh in heel region

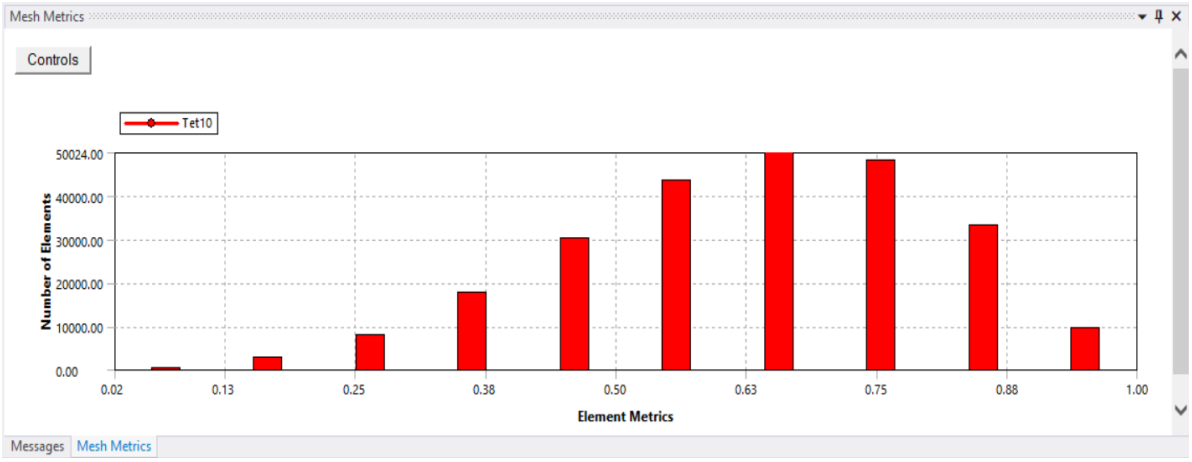

Figure 4-4 Graph representing quantity of elements falling in percentage quality of mesh elements

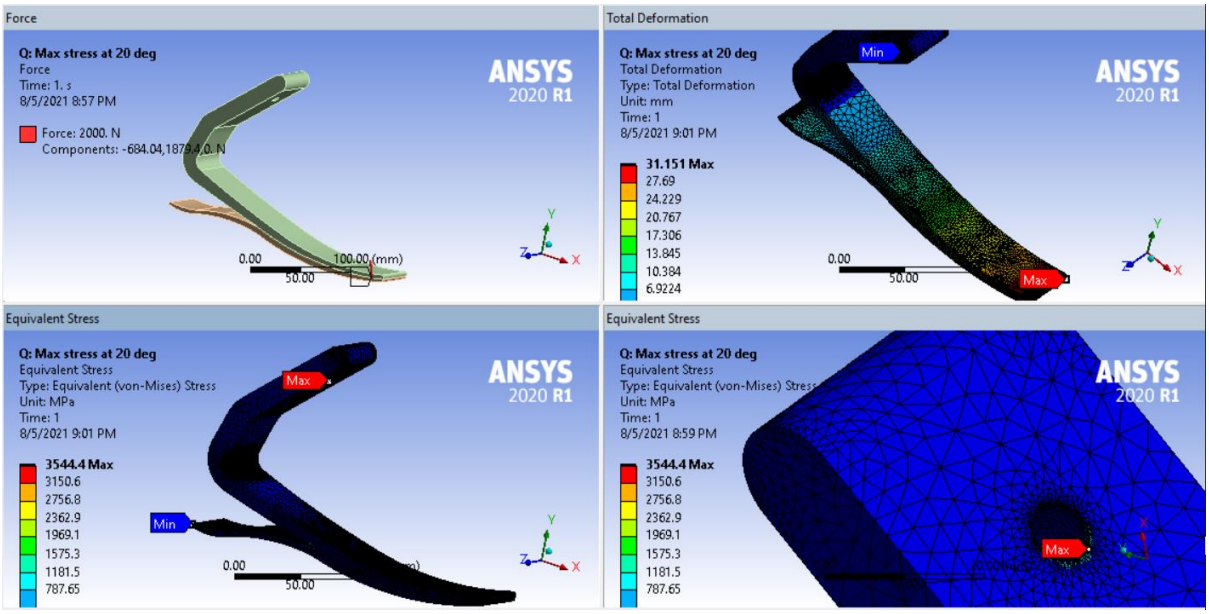

Figure 4-5 Maximum deflection and equivalent stress in toe region upon application of 2000N force

As discussed, cyclic testing procedure is adopted as per mentioned in the literature in [48]. Forces at critical data points are applied on heel and toe region of model developed and corresponding values of maximum deflection is tabulated to form graphs. Figure 4-7 and Figure 4-8 shows the graph representing the maximum deflection against the increasing force applied in both hip and toe region, one at a time. The graph depicts almost linear behaviour of deflection when an incremental force is applied at specified angle. Behaviour of prosthesis is evaluated using the M curve mentioned in ISO 22675. It means that the behaviour of deflection should be according to the force applied in M-curve at given angles. This implies that maximum deflection values at specified angles and applied force recorded during

analysis are used to find the behaviour of maximum deflection in heel and toe region against stance time as indicated in figure 4-9.

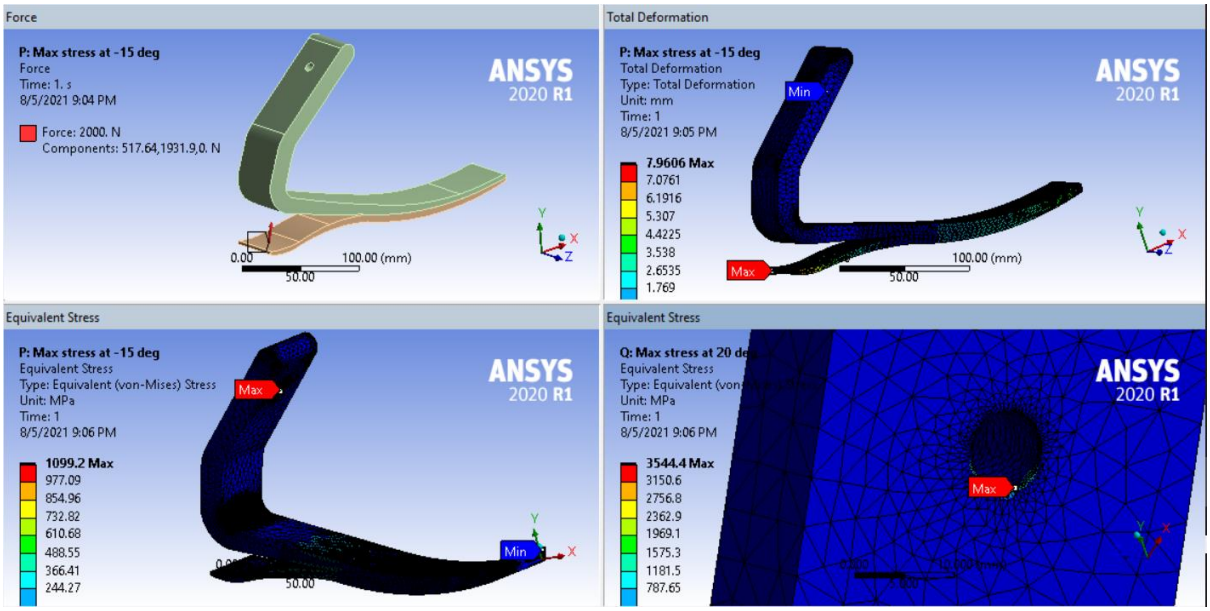

Figure 4-6 Maximum deflection and equivalent stress in heel region upon application of 2000N force

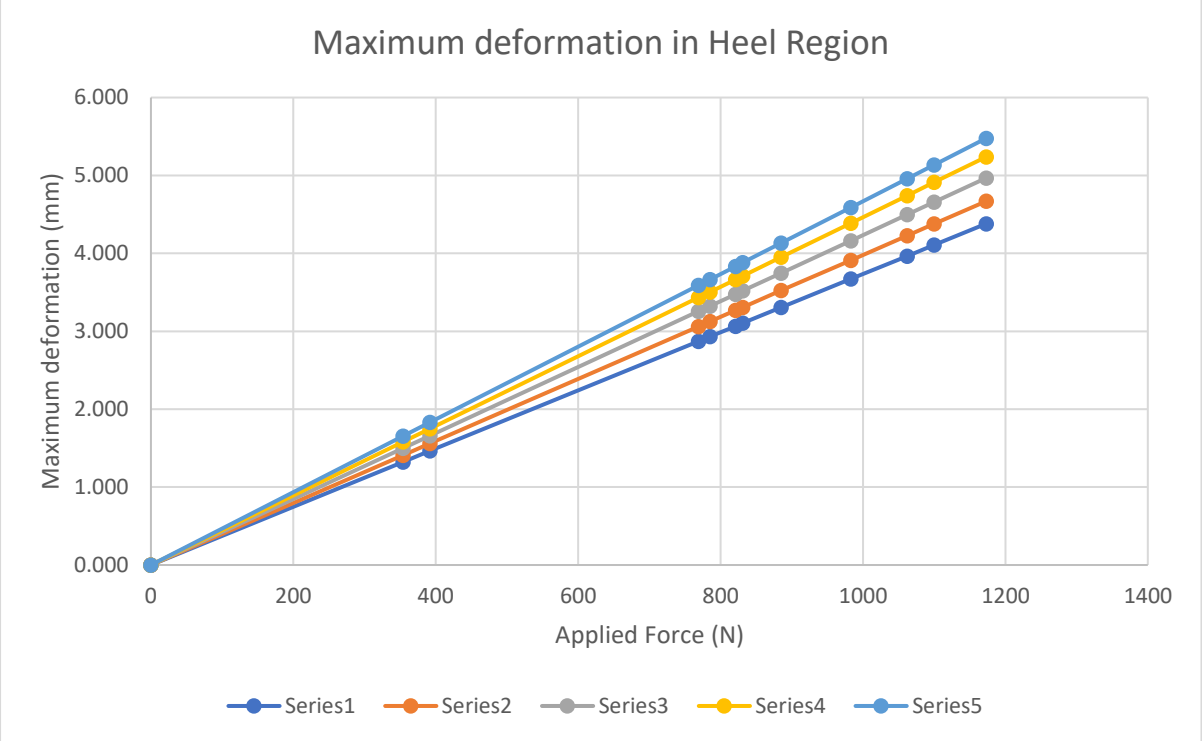

Figure 4-7 Maximum deformation in heel region upon application of critical point load

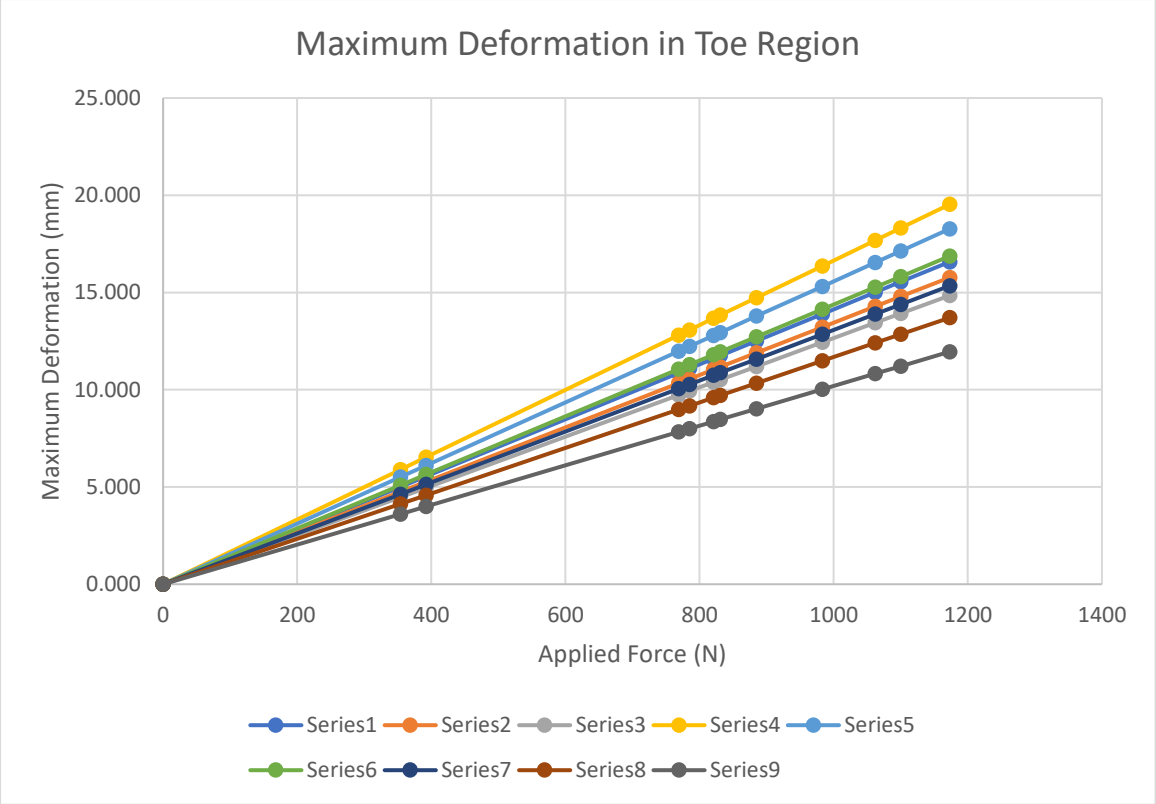

Figure 4-8 Maximum deformation in toe region upon application of critical point load

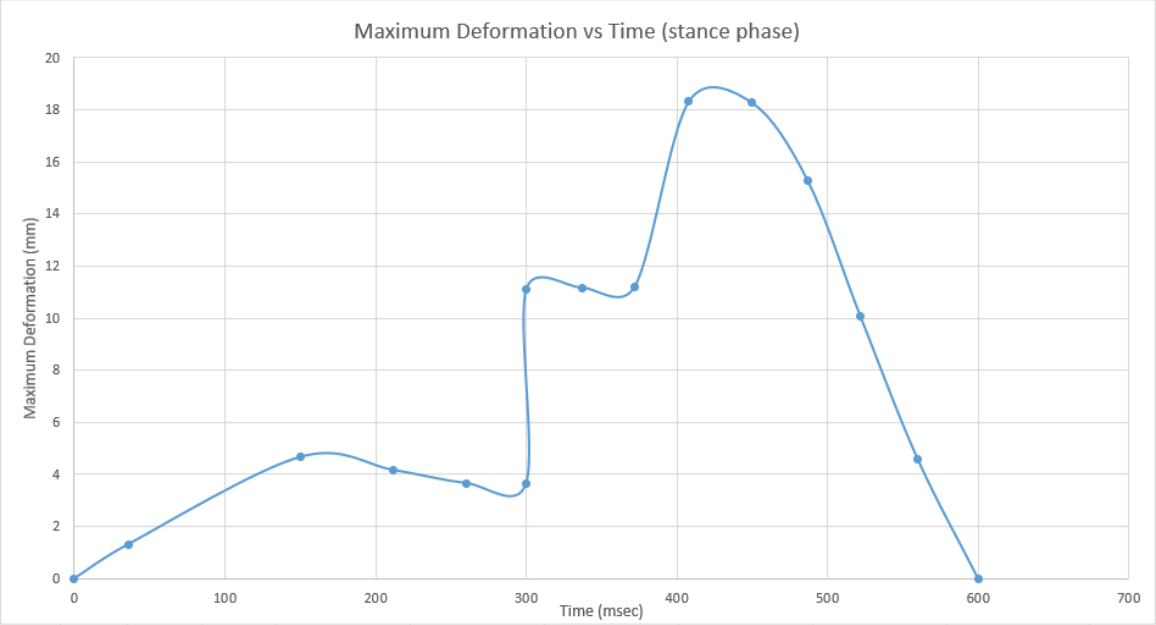

Figure 4-9 Maximum deformation of heel and toe region in stance phase

4.5 Discussion

As discussed earlier in this chapter, this methodology had been adopted in literature for CEME developed foot prosthesis [48]. The researcher obtained maximum displacement in both heel and toe region and compare results with Niagara foot prosthesis obtained in [20]. Considering same methodology, the analysis metrics developed for this research is shown in Table 4-3.

Table 4-3 Comparison of results with benchmarks

Parameters	**Desired Value**	**Achieved Value CEME foot**	**Achieved Value in thesis**
Maximum displacement in heel contact	9 mm	10 mm	5.477 mm
Maximum displacement in toe contact	40 mm	34mm	19.531mm

The values of maximum displacement have been plotted against stance phase time during which the foot is in contact with the ground as shown in figure 4-10. The behaviour of the maximum displacement curve in heel and toe regions resembles with lower achieved value of maximum displacement during the simulation of prosthesis designed. The maximum value of displacement achieved during the heel contact and toe contact are 5.477mm and 19.531mm respectively. This indicates conformance of foot prosthesis used in this thesis comparing to Niagara foot and CEME developed foot prosthesis considering the maximum displacement values.

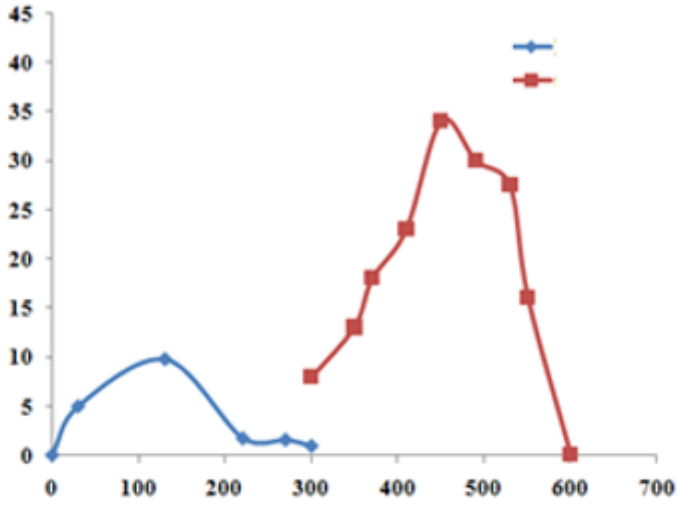

(a)

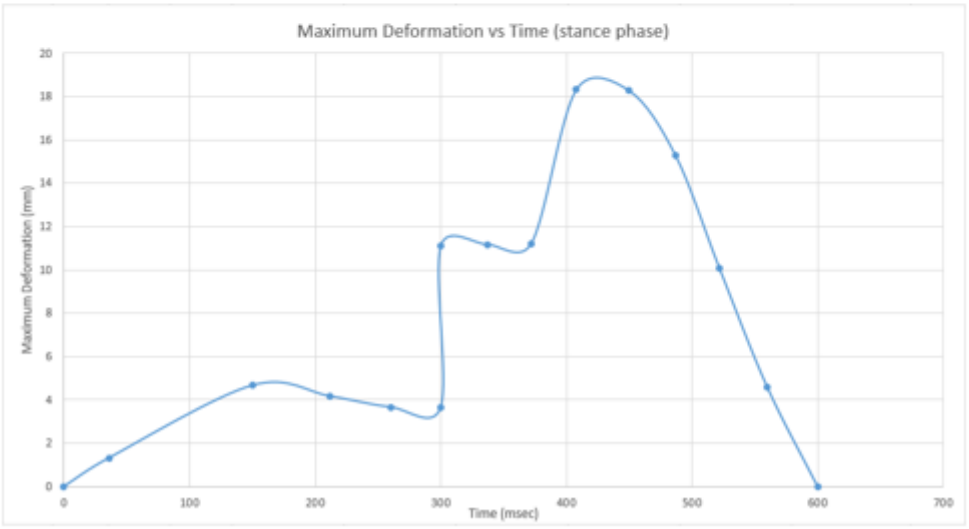

(b)

Figure 4-10 comparing maximum displacement of heel and toe region (a) results of CEME foot (b) results of this thesis

CHAPTER 5: CONCLUSION AND FURTURE WORK

5.1 Conclusion

A 2 DOF test robot for gait and cyclic testing of lower limb prosthesis is fabricated. An extensive literature review is performed in understanding the behavior of lower limb prosthesis and testing criteria adopted by the researchers in manufacturing both transfemoral and transtibial prosthesis. Furthermore, the design parameters and features for testing platforms and mechanisms have been studied in detail and a CAD model is developed for fabrication and simulation of human gait. The CAD model is imported in MATLAB Simscape® for simulation of human gait.

A methodology for the fabrication of test bench for transfemoral prosthesis is adopted. The values of linear carriage and rotary actuator are calculated and motors and drive system for the actuators are procured. The assembly of the actuators are fabricated in accordance with model and design techniques and a mechanical structure of a test bench is developed. Servo motors and drives are selected for providing position control to the system and a power distribution board is developed to provide necessary power to the system as well halt the actuator in-case of an alarm generation or emergency.

Moreover, a foot prosthesis is designed in solidworks® considering Sierra® foot prosthesis model and cyclic durability testing is performed using FEM technique. The model of foot prosthesis is imported to Ansys Workbench® and maximum deflections in heel and toe regions are calculated using forces against critical data points extracted from ISO 22675 cyclic durability test curve. This curve represents the Vertical Ground Reaction Force (vGRF) that human being produces during the stance phase of the gait cycle. The maximum deflections of heel and toe regions are plotted against the stance phase time which are evaluated against deflection in Niagara foot prosthesis stated in the literature.

5.2 Future Work

A transfemoral prosthesis test bench is designed to replicate hip vertical motion and thigh rotational motion. Treadmill is used as a running platform to perform moving surface the system enabling the test bench to perform cyclic testing of both transfemoral and transtibial prosthesis. The test bench has the capability to perform cyclic testing of all types of lower limb prosthesis, provided the mounting assemblies are provided as per designed variable height shank.

The weight of the housing for thigh rotational motion is limitation of system that needs to be catered. The housing weighs 14.7 Kg and the mounting sheet on which housing is mounted is 6.4 kgs. It can be reduced using composite materials to increase the speed of the system. Using composite materials such as carbon fiber, this weight can be reduced which will tends to reduce the overall weight of the carriage. The motor can bear an axial load of 14.7 Kg and by changing the material of the housing the carriage can be reduced to conform the axial load of the system. This will help in removing the 5:1 gearbox provided to the system eventually reducing load to motor inertia ratio of the system. However, the cost of manufacturing will increase.

The machine is designed and fabricated considering a cost-effective solution for industrial and medical use. The vertical slider comprises of bushes drive system generally used in lath machines for slow movements. These bushes are made of rubber material and have high frictional coefficient that increases the required load torque to drive the vertical carriage. Load torque can be reduced by reducing the frictional force of the system; the torque can be reduce using roller sliding mechanism. The treadmill used for the system has the tendency to provide inclination in angles that can provide results of behavior of prosthesis during walking on inclined surfaces. The torques produce for the system in this case, will be higher during climbing the endurance of the system can be judged during inclined surfaces.

The foot prosthesis used for cyclic durability testing indicates conformance of foot with respect to displacements in heel and toe region. Furthermore, the energy storing capacity of foot prosthesis be analyzed to access the capability of foot to retain energy in early stance phase and provide propulsion to the user in later stance phase (toe-off region).

APPENDIX A

Using Servo Motors

(1) Specifications and Operating Conditions of the Drive Mechanism

A servo motor for driving a single-axis table is selected, as shown in the figure below.

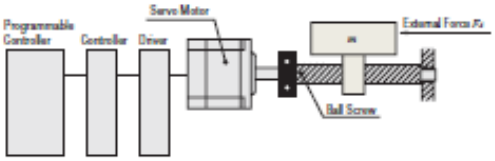

Max. speed of table ..... $V_L = 0.2$ [m/s]
Resolution ..... $\Delta l = 0.02$ [m/s]
Motor power supply ..... Single-Phase 115 VAC
Total mass of table and load ..... $m = 100$ [kg]
External force ..... $F_A = 29.4$ [N]
Friction coefficient of sliding surface ..... $\mu = 0.04$
Efficiency of ball screw ..... $\eta = 0.9$
Internal friction coefficient of preload nut ..... $\mu_B = 0.3$
Ball screw shaft diameter ..... $D_B = 25$ [mm]
Total length of ball screw ..... $L_B = 1000$ [mm]
Ball screw lead ..... $P_B = 10$ [mm]
Ball screw material ..... Iron (density $\rho = 7.9 \times 10^3$ [kg/m^3])
Operating cycle ... Operation for 2.1 sec./stopped for 0.4 sec. (repeated)
Acceleration/deceleration time ..... $t_1 = t_2 = 0.1$ [s]

(2) Calculation of the Required Resolution θ

The resolution of the motor is calculated from the resolution required to drive the table.

$$\theta = \frac{360^\circ \cdot \Delta l}{P_B} = \frac{360^\circ \times 0.02}{10} = 0.72^\circ$$

The resolution of the **NX** series, $\theta_M = 0.36^\circ$/pulse, satisfies this condition.

(3) Determination of Operating Pattern

The motor speed N_M is calculated using the following formula.

$$N_M = \frac{60 \cdot V_L}{P_B} = \frac{60 \times 0.2}{10 \times 10^{-3}} = 1200 \text{ [r/min]}$$

A speed pattern is created from this N_M and operating cycle, as well as the acceleration/deceleration time.

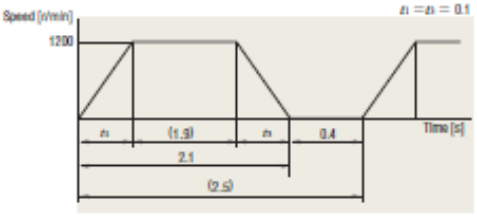

(4) Calculation of Load Torque T_L [N·m]

Force of moving direction $F = F_A + m \cdot g (\sin\theta + \mu \cdot \cos\theta)$
$= 29.4 + 100 \times 9.807 (\sin 0^\circ + 0.04 \cos 0^\circ)$
$= 68.6$ [N]

Load torque of motor shaft conversion

$$T_L = \frac{F \cdot P_B}{2\pi \cdot \eta} + \frac{\mu_B \cdot F_A \cdot P_B}{2\pi}$$

$$= \frac{68.6 \times 10 \times 10^{-3}}{2\pi \times 0.9} + \frac{0.3 \times 22.9 \times 10 \times 10^{-3}}{2\pi}$$

$\fallingdotseq 0.13$ [N·m]

Here, the ball screw preload $F_B = \frac{1}{3} F$.

(5) Calculation of Load Inertia J_L [kg·m^2]

Inertia of ball screw

$$J_B = \frac{\pi}{32} \cdot \rho \cdot L_B \cdot D_B^4$$

$$= \frac{\pi}{32} \times 7.9 \times 10^3 \times 1000 \times 10^{-3} \times (25 \times 10^{-3})^4$$

$\fallingdotseq 3.03 \times 10^{-4}$ [kg·m^2]

Inertia of table and work $J_W = m \left(\frac{P_B}{2\pi}\right)^2$

$$= 100 \times \left(\frac{10 \times 10^{-3}}{2\pi}\right)^2$$

$\fallingdotseq 2.53 \times 10^{-4}$ [kg·m^2]

Load inertia $J_L = J_B + J_W$
$= 3.03 \times 10^{-4} + 2.53 \times 10^{-4} = 5.56 \times 10^{-4}$ [kg·m^2]

(6) Tentative Selection of Servo Motor

Safety factor $S_f = 1.5$

Load torque $T_L = S_f \cdot T_L$
$= 1.5 \times 0.13 = 0.195$ [N·m]

Load inertia $J_L = 5.56 \times 10^{-4}$ [kg·m^2]

This gives us a speed of 1200 [r/min], and a rated torque of 0.195 [N·m] or higher is output. A servo motor with a permissible load inertia of 5.56×10^{-4} [kg·m^2] or higher is selected.

→ NX620AA-3

Rated speed $N = 3000$ [r/min]
Rated torque $T_M = 0.637$ [N·m]
Rotor inertia $J_R = 0.162 \times 10^{-4}$ [kg·m^2]
Permissible load inertia $J = 8.1 \times 10^{-4}$ [kg·m^2]
Maximum instantaneous torque $T_{MAX} = 1.91$ [N·m]
The above values are appropriate.

(7) Calculation of Acceleration Torque T_A [N·m] and Deceleration Torque T_D [N·m]

Acceleration/deceleration torque is calculated using the following formula.

$$T_A = (T_D) = \frac{(J_L + J_R) N_M}{9.55 t_1}$$

$$= \frac{(5.56 \times 10^{-4} + 0.162 \times 10^{-4}) \times 1200}{9.55 \times 0.1} \fallingdotseq 0.72 \text{ [N·m]}$$

(8) Calculation of Required Torque T [N·m]

$T = T_M + T_L$
$= 0.72 + 0.13 = 0.85$ [N·m]

This required torque can be used with **NX620AA-3** in order to keep the maximum instantaneous torque of **NX620AA-3** at 1.91 [N·m] or less.

(9) Determination of Torque Pattern

The torque pattern is determined with the operating cycle, acceleration/deceleration torque, load torque and acceleration time.

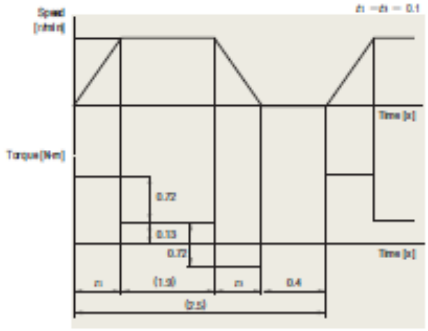

(10) Calculation of Effective Load Torque T_{rms} [N·m]

The effective load torque T_{rms} is determined with the torque pattern and the following formula.

$$T_{rms} = \sqrt{\frac{(T_a + T_L)^2 \cdot t_1 + T_L^2 \cdot t_2 + (T_d - T_L)^2 \cdot t_3}{t_T}}$$

$$= \sqrt{\frac{(0.72 + 0.13)^2 \times 0.1 + 0.13^2 \times 1.9 + (0.72 - 0.13)^2 \times 0.1}{2.5}}$$

$\fallingdotseq 0.24$ [N·m]

Here, from the operating cycle, $t_1 + t_2 + t_3 = 2.1$ [s] and the acceleration/deceleration time $t_1 = t_3 = 0.1$. Based on this, $t_2 = 2.1 - 0.1 \times 2 = 1.9$ [s].
The ratio between this T_{rms} and the rated torque T_M of the servo motor (the effective load safety factor) is determined with the following formula.

$$\frac{T_M}{T_{rms}} = \frac{0.637}{0.24} = 2.65$$

In general, a motor can operate at an effective load safety factor of 1.5 to 2.

Using Standard AC Motors

(1) Specifications and Operating Conditions of the Drive Mechanism

This selection example demonstrates an electromagnetic brake motor for use on a table moving vertically on a ball screw.
In this case, a motor must be selected that meets the following required specifications.

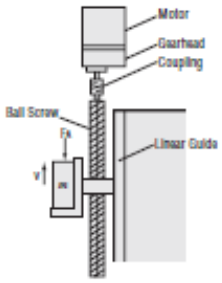

Total mass of the table and load ..... $m = 45$ [kg]
Table speed ..... $V = 15 \pm 2$ [mm/s]
External force ..... $F_A = 0$ [N]
Ball screw tilt angle ..... $\alpha = 90$ [deg]
Total length of ball screw ..... $L_B = 800$ [mm]
Ball screw shaft diameter ..... $D_B = 20$ [mm]
Ball screw lead ..... $P_B = 5$ [mm]
Distance moved for one rotation of ball screw ..... $A = 5$ [mm]
Ball screw efficiency ..... $\eta = 0.9$
Ball screw material ..... Iron (density $\rho = 7.9 \times 10^3$ [kg/m^3])
Internal friction coefficient of preload nut ..... $\mu_B = 0.3$
Friction coefficient of sliding surface ..... $\mu = 0.05$
Motor power supply ..... Single-Phase 115 VAC 60 Hz
Operating time ..... Intermittent operation, 5 hours/day
Load with repeated starts and stops
Required load holding

(2) Determine the Gear Ratio

Speed at the gearhead output shaft $N_G = \frac{V \cdot 60}{A} = \frac{(15 \pm 2) \times 60}{5}$

$= 180 \pm 24$ [r/min]

Because the rated speed for a 4-pole motor at 60 Hz is 1450 to 1550 r/min, the gear ratio is calculated as follows:

Gear ratio $i = \frac{1450 \sim 1550}{N_G} = \frac{1450 \sim 1550}{180 \pm 24} = 7.1 \sim 9.9$

This gives us a gear ratio of $i = 9$.

(3) Calculate the Required Torque T_M [N·m]

Force of moving direction $F = F_A + m \cdot g (\sin\theta + \mu \cdot \cos\theta)$

$= 0 + 45 \times 9.807 (\sin 90^\circ + 0.05 \cos 90^\circ)$

$= 441$ [N]

Ball screw preload $F_B = \frac{F}{3} = 147$ [N]

Load torque $T_L = \frac{F \cdot P_B}{2\pi\eta} + \frac{\mu_B \cdot F_B \cdot P_B}{2\pi}$

$= \frac{441 \times 5 \times 10^{-3}}{2\pi \times 0.9} + \frac{0.3 \times 147 \times 5 \times 10^{-3}}{2\pi}$

$= 0.426$ [N·m]

Allow for a safety factor of 2 times.

$T_L = T_L \cdot 2 = 0.426 \times 2 = 0.86$ [N·m]

APPENDIX B

Parameters for Vertical Motor Selection

```
clc;
clear;

Total_Mass= 120;              % Total mass of driven system
in Kg.
Max_Linear_Speed= 1;          % design speed in mm/s
F_A= 80;                      % Frictional Force in N
alpha = 90;                   % Ball screw tilt angle in
deg  .
B_S_length = 1;               % Ball Screw Length in m.
Guide_Travel = 0.300;         % total span of travel in m
B_S_Dia= 0.032;               % Ball Screw Diameter in m
B_S_lead = 0.010;             % Ball Screw pitch/lead in m
B_S_eff= 0.8;                 % Ball Screw efficiency
B_S_density = 7500;           % Ball Screw Density in kg/m3
meu_not = 0.2;                % Internal friction
coefficient of preload nut;
meu = 0.05;                   % Friction coefficient of
sliding surface;
Oper_Voltage= 220;            % Motor power supply voltage;
Oper_freq= 50;                % Motor power supply
frequency;
Oper_Time = 5;                % Time of operation in hours
/day;
g = 9.807;                    % gravitational Acceleration

Safety_Factor = 2;
gearbox_eff = 0.86;
Motor_rated_speed = 3000;     % Rated Speed in Rev/min
```

CALCULATION CODE

```
% calculation relative to max speed
% calculating the angular speed of the Ball screw in
Rev/Min
B_S_speed = (Max_Linear_Speed*60)/B_S_lead;

% calculating Required Gear Ratio considering speed
i = Motor_rated_speed / B_S_speed;
i_prime=5;
```

```
% Torque Calculations
% Force(N) required to move 120kg mass
Force = F_A + ((Total_Mass *
g)*(sin(alpha)+(meu*cos(alpha))));
% the preload force of ball screw F0
B_S_preload=Force/3;
Load_Torque=
((Force*B_S_lead)/(2*pi*B_S_eff))+((meu_not*B_S_preload*B
_S_lead)/2*pi);
Safe_torque= Load_Torque*Safety_Factor;

% calculating Required Motor Torque considering gearbox
Motor_torque = Safe_torque/(i_prime*gearbox_eff)

%Estimating load inertia of the vertical mechanism
%calculating Ball screw inertia
B_S_Inertia = (pi/32)*B_S_length*B_S_density*(B_S_Dia^4);
%calculating inertia of slider and load
Load_inertia = Total_Mass*((B_S_lead/20*pi)^2);
Inertia= Load_inertia + B_S_Inertia
M_G_inertia = 0.000143;
Gear_inertia = M_G_inertia*(i_prime^2)

Ratio_L_M_Inertia = Inertia/Gear_inertia
%Ratio_L_M_Inertia = Inertia/M_G_inertia
```

RESULTS

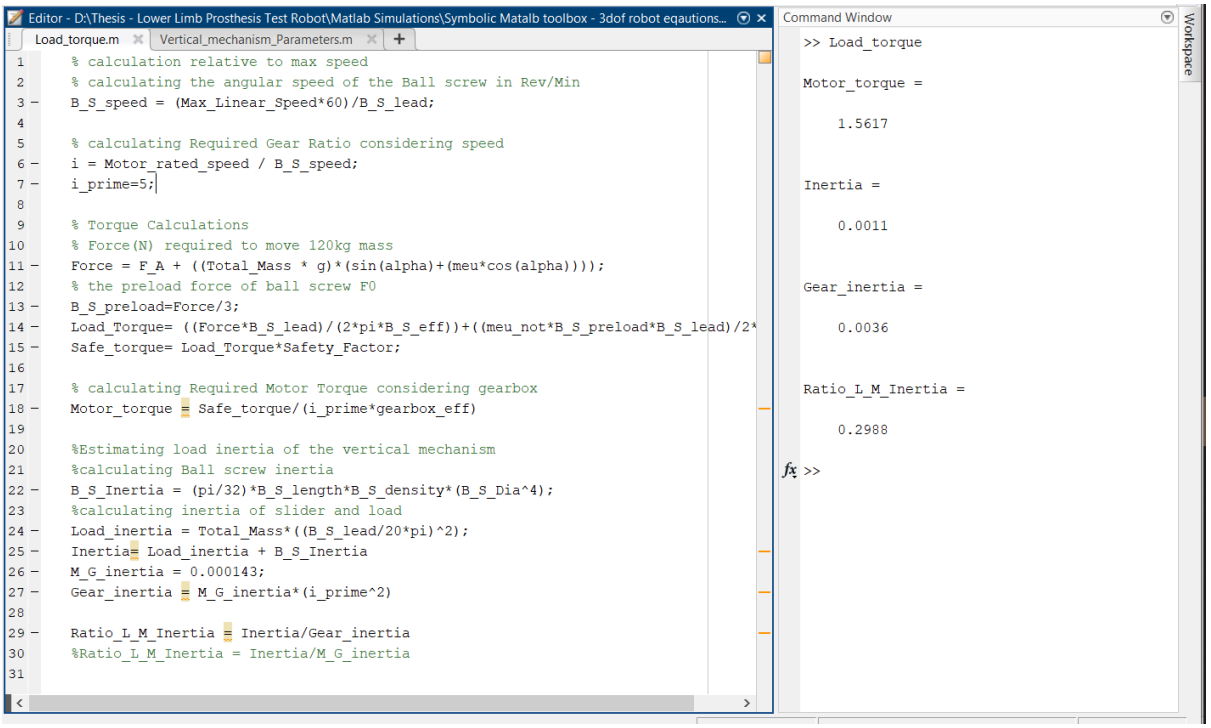

APPENDIX C

MOTOR SPECIFICATIONS

Item \ Servo motor			HF-MP series (Ultra-low inertia · small capacity)					HF-KP series (Low inertia · small capacity)				
			053	13	23	43	73	053	13	23	43	73
Applicable servo amplifier/drive unit	MR-J3-□A/B/B-RJ006/T		10		20	40	70	10		20	40	70
	MR-J3-□A1/B1/B1-RJ006/T1		10		20	40		10		20	40	
Continuous running duty (Note 1)	Rated output	[kW]	0.05	0.1	0.2	0.4	0.75	0.05	0.1	0.2	0.4	0.75
	Rated torque	[N · m]	0.16	0.32	0.64	1.3	2.4	0.16	0.32	0.64	1.3	2.4
		[oz · in]	22.7	45.3	90.6	184	340	22.7	45.3	90.6	184	340
Rated speed (Note 1)		[r/min]	3000					3000				
Maximum speed (Note 10)		[r/min]	6000					6000				
Instantaneous permissible speed		[r/min]	6900					6900				
Maximum torque Values in parentheses are at the maximum torque of 350% (note 11)		[N · m]	0.48	0.95	1.9	3.8	7.2	0.48 (0.56)	0.95 (1.11)	1.9 (2.23)	3.8 (4.46)	7.2 (8.36)
		[oz · in]	68.0	135	269	538	1020	68.0 (79.3)	135 (157)	269 (316)	538 (632)	1020 (1180)
Power rate at continuous rated torque		[kW/s]	13.3	31.7	46.1	111.6	95.5	4.87	11.5	16.9	38.6	39.9
Inertia moment (Note 3)	J	[×10^{-4}kg · m^2]	0.019	0.032	0.088	0.15	0.60	0.052	0.088	0.24	0.42	1.43
	WK^2	[oz · in^2]	0.104	0.175	0.481	0.82	3.28	0.284	0.481	1.31	2.30	7.82
Recommended ratio of load inertia moment to servo motor shaft inertia moment (Note 2, 10)			30 times or less					15 times or less		24 times or less	22 times or less	15 times or less
Power supply capacity			Refer to "Power supply equipment capacity and generated loss of servo amplifiers" in Servo Amplifier Instruction Manual.									
Rated current		[A]	1.1	0.9	1.6	2.7	5.6	0.9	0.8	1.4	2.7	5.2
Maximum current Values in parentheses are at the maximum torque of 350% (note 11)		[A]	3.2	2.8	5.0	8.6	16.7	2.7 (3.1)	2.4 (2.8)	4.2 (4.9)	8.1 (9.5)	15.6 (18.2)
Speed/position detector			Encoder common to absolute position and incremental detection systems (Resolution per servo motor 1 rotation: 262144pulse/rev)									
Accessory												
Insulation class			130(B)									
Structure			Totally - enclosed, natural-cooling (IP rating: IP65 (Note 4, 9))									
Environmental conditions (Note 5)	Ambient temperature	Operation [°C]	0 to 40 (non-freezing)									
		Operation [°F]	32 to 104 (non-freezing)									
		Storage [°C]	−15 to 70 (non-freezing)									
		Storage [°F]	5 to 158 (non-freezing)									
	Ambient humidity	Operation	10 to 80%RH (non-condensing)									
		Storage	10 to 90%RH (non-condensing)									
	Ambience		Indoors (no direct sunlight) Free from corrosive gas, flammable gas, oil mist, dust and dirt.									
	Altitude		Max.1000m above sea level									
	Vibration resistance (Note 6)	[m/s^2]	X, Y: 49									
Vibration rank (Note 7)			V10									
Permissible load for the shaft (Note 8, 10)	L	[mm]	25		30		40	25		30		40
	Radial	[N]	88		245		392	88		245		392
		[lb]	19.8		55.1		88.1	19.8		55.1		88.1
	Thrust	[N]	59		98		147	59		98		147
		[lb]	13.3		22.0		33.0	13.3		22.0		33.0
Mass (Note 3)		[kg]	0.35	0.56	0.94	1.5	2.9	0.35	0.56	0.94	1.5	2.9
		[lb]	0.77	1.24	2.07	3.31	6.39	0.77	1.24	2.07	3.31	6.39

APPENDIX D

POWER BOARD LOGIC AS PER MANUAL

3.2.1 Position control mode

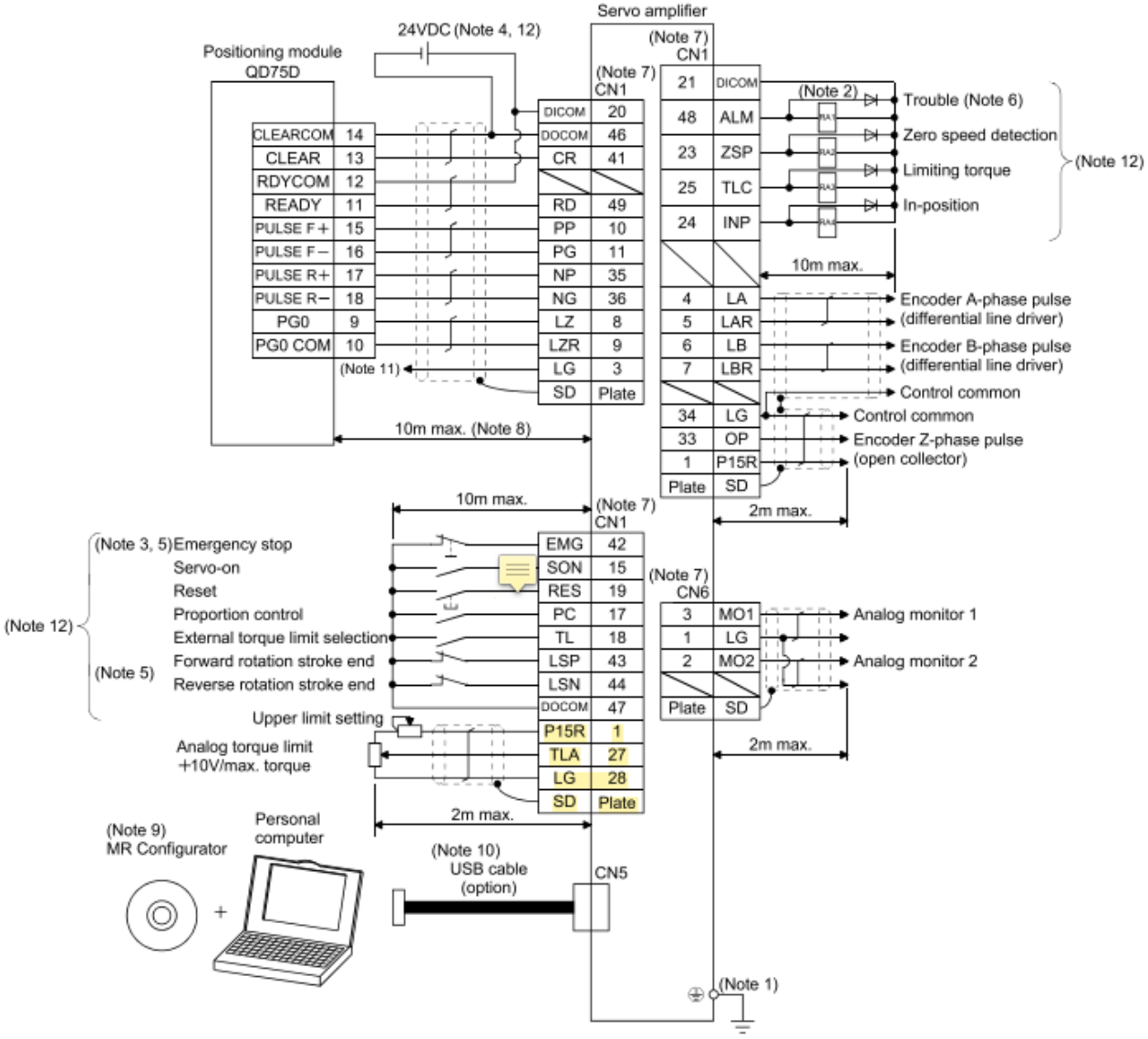

APPENDIX E

LAYOUT PLAN

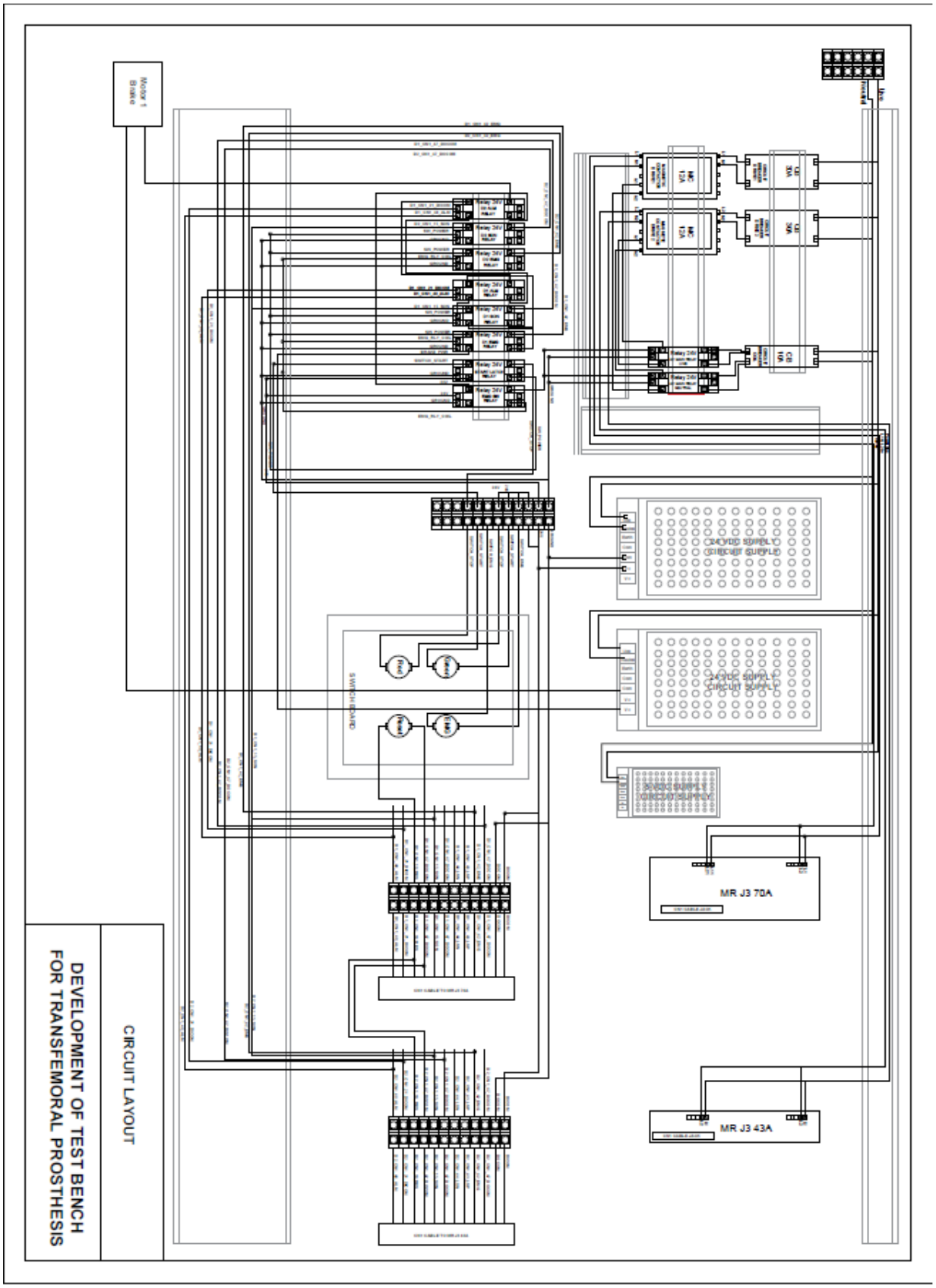

APPENDIX F

Simscape Model for Simulation

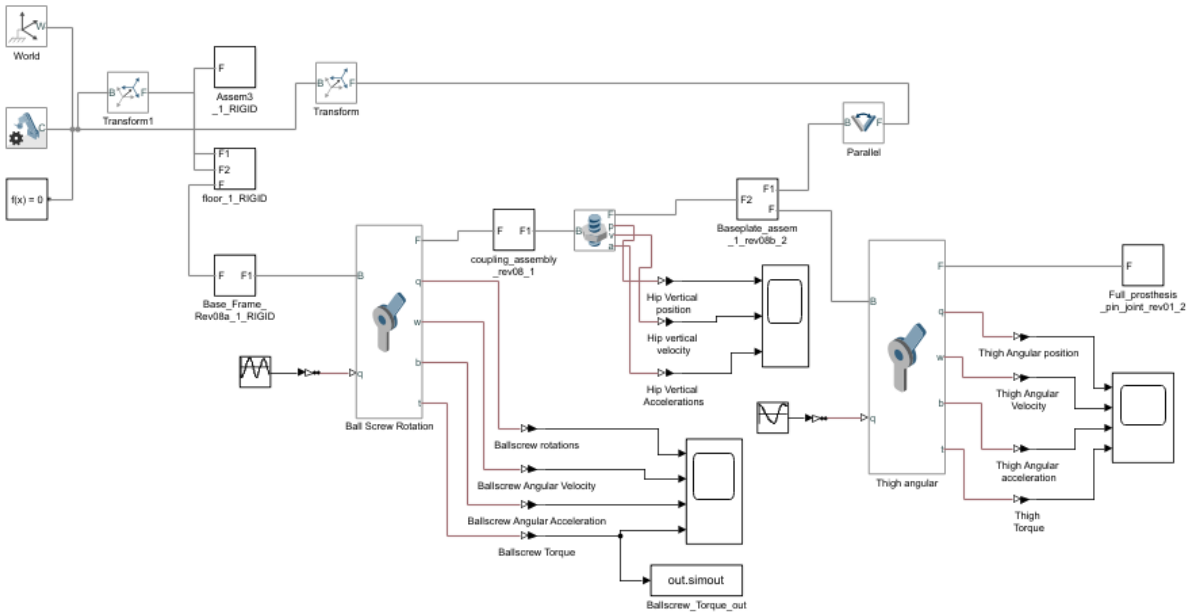

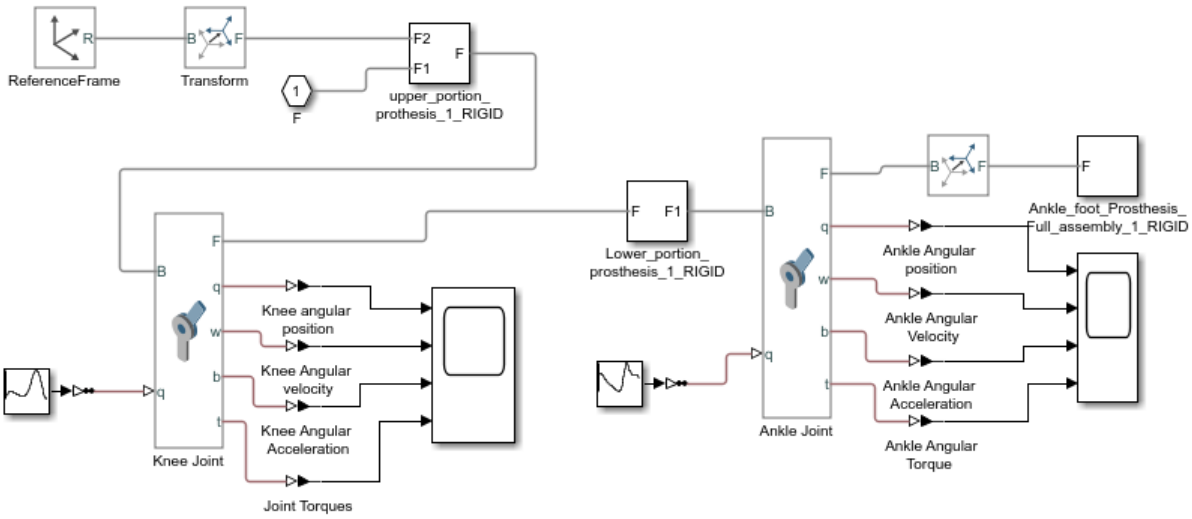

REFERENCES

[1] L. Flynn, J. Geeroms, R. Jimenez-Fabian, B. Vanderborght, N. Vitiello, and D. Lefeber, "Ankle-knee prosthesis with active ankle and energy transfer: Development of the CYBERLEGs Alpha-Prosthesis," *Rob. Auton. Syst.*, vol. 73, pp. 4–15, 2015, doi: 10.1016/j.robot.2014.12.013.

[2] S. Ozkan, "The causes and levels of lower limb amputation in geriatric patients," vol. 28, no. 5, pp. 893–896, 2021, doi: 10.5455/annalsmedres.2020.05.508.

[3] N. Ahmad, G. N. Thomas, P. Gill, C. Chan, and F. Torella, "Lower limb amputation in England: prevalence, regional variation and relationship with revascularisation, deprivation and risk factors. A retrospective review of hospital data," *J. R. Soc. Med.*, vol. 107, no. 12, pp. 483–489, 2014, doi: 10.1177/0141076814557301.

[4] B. Imam, W. C. Miller, H. C. Finlayson, J. J. Eng, and T. Jarus, "Incidence of lower limb amputation in Canada," *Can. J. Public Heal.*, vol. 108, no. 4, pp. e374–e380, 2017, doi: 10.17269/cjph.108.6093.

[5] C.-A. Behrendt *et al.*, "International Variations in Amputation Practice: A VASCUNET Report," *J. Vasc. Surg.*, vol. 68, no. 4, pp. 1275–1276, 2018, doi: 10.1016/j.jvs.2018.08.008.

[6] M. Moini, M. R. Rasouli, A. Khaji, F. Farshidfar, and P. Heidari, "Patterns of extremity traumas leading to amputation in Iran: Results of Iranian National Trauma Project," *Chinese J. Traumatol. - English Ed.*, vol. 12, no. 2, pp. 77–80, 2009, doi: 10.3760/cma.j.issn.1008-1275.2009.02.003.

[7] A. Rouhani and S. Mohajerzadeh, "An epidemiological and etiological report on lower extremity amputation in northwest of Iran," *Arch. Bone Jt. Surg.*, vol. 1, no. 2, pp. 103–106, 2013, doi: 10.22038/abjs.2013.2083.

[8] J. Shaw *et al.*, "Quality of life and complications in lower limb amputees in Tanzania: results from a pilot study," *Lancet Glob. Heal.*, vol. 6, p. S18, 2018, doi: 10.1016/s2214-109x(18)30147-5.

[9] E. G. Krug, G. K. Sharma, and R. Lozano, "The global burden of injuries," *Am. J. Public Health*, vol. 90, no. 4, pp. 523–526, 2000, doi: 10.2105/AJPH.90.4.523.

[10] C. L. McDonald, S. Westcott-McCoy, M. R. Weaver, J. Haagsma, and D. Kartin, "Global prevalence of traumatic non-fatal limb amputation," *Prosthet. Orthot. Int.*, 2020, doi: 10.1177/0309364620972258.

[11] P. Shankar, V. S. Grewal, S. Agrawal, and S. V Nair, "ScienceDirect A study on quality of life among lower limb amputees at a tertiary prosthetic rehabilitation center," *Med. J. Armed Forces India*, vol. 76, no. 1, pp. 89–94, 2018, doi: 10.1016/j.mjafi.2019.02.008.

[12] C. Marshall and G. Stansby, "Amputation and rehabilitation," *Surgery*, vol. 28, no. 6, pp. 284–287, 2010, doi: 10.1016/j.mpsur.2010.01.017.

[13] I. Gaunaurd, A. Kristal, A. Horn, C. Krueger, O. Muro, and A. Rosenberg, "The Utility of the Two-Minute Walk Test as a Measure of Mobility in People with Lower Limb Amputation," *Arch. Phys. Med. Rehabil.*, 2020, doi: 10.1016/j.apmr.2020.03.007.

[14] G. I. Lopez-Avina, E. Barocio, and J. C. Huegel, "Pseudo fatigue test of passive energy-returning prosthetic foot," *GHTC 2017 - IEEE Glob. Humanit. Technol. Conf. Proc.*, vol. 2017-Janua, pp. 1–7, 2017, doi: 10.1109/GHTC.2017.8239315.

[15] H. Tryggvason, F. Starker, C. Lecomte, and F. Jonsdottir, "Use of dynamic FEA for design modification and energy analysis of a variable stiffness prosthetic foot," *Appl. Sci.*, vol. 10, no. 2, 2020, doi: 10.3390/app10020650.

[16] M. Hamzah and A. Gatta, "Design of a Novel Carbon-Fiber Ankle-Foot Prosthetic

using Finite Element Modeling," *IOP Conf. Ser. Mater. Sci. Eng.*, vol. 433, no. 1, 2018, doi: 10.1088/1757-899X/433/1/012056.
[17] S. Lapapong, S. Sucharitpwatskul, N. Pitaksapsin, C. Srisurangkul, S. Lerspalungsanti, and R. Naewngerndee, "Finite element modeling and validation of a four-bar linkage prosthetic knee under static and cyclic strength tests," *i-CREATe 2013 - Int. Conv. Rehabil. Eng. Assist. Technol. Conjunction with SENDEX 2013*, vol. 6824, 2013, doi: 10.3402/jartt.v2.23211.
[18] H. Richter, D. Simon, W. A. Smith, and S. Samorezov, "Dynamic modeling, parameter estimation and control of a leg prosthesis test robot," *Appl. Math. Model.*, vol. 39, no. 2, pp. 559–573, 2015, doi: 10.1016/j.apm.2014.06.006.
[19] I. Díaz, J. J. Gil, and E. Sánchez, "Lower-Limb Robotic Rehabilitation: Literature Review and Challenges," *J. Robot.*, vol. 2011, no. i, pp. 1–11, 2011, doi: 10.1155/2011/759764.
[20] A. Haberman, "Mechanical Properties of Dynamic Energy Return Prosthetic Feet," p. 130, 2008.
[21] L. E. Thorp, "Hip Anatomy," pp. 3–15, 2015, doi: 10.1007/978-1-4614-6965-0.
[22] M. Miller and S. Thompson, "Knee Anatomy and Biomechanics of the Knee," *DeLee Drez's Orthop. Sport. Med.*, vol. 11, no. 3, pp. 1047–1072, 2014, doi: 10.1053/otsm.
[23] L. D. Noble, R. W. Colbrunn, D. G. Lee, A. J. Van Den Bogert, and B. L. Davis, "Design and validation of a general purpose robotic testing system for musculoskeletal applications," *J. Biomech. Eng.*, vol. 132, no. 2, 2010, doi: 10.1115/1.4000851.
[24] C. Marinelli, H. Giberti, and F. Resta, "In vitro test method for the development of intelligent lower limb prosthetic devices," *Biocybern. Biomed. Eng.*, vol. 37, no. 1, pp. 11–23, 2017, doi: 10.1016/j.bbe.2016.10.003.
[25] V. Rajťúková, M. Michalíková, L. Bednarcíková, A. Balogová, and J. Živčák, "Biomechanics of lower limb prostheses," *Procedia Eng.*, vol. 96, pp. 382–391, 2014, doi: 10.1016/j.proeng.2014.12.107.
[26] A. S. Alharthi, S. U. Yunas, and K. B. Ozanyan, "Deep learning for monitoring of human gait: A review," *IEEE Sens. J.*, vol. 19, no. 21, pp. 9575–9591, 2019, doi: 10.1109/JSEN.2019.2928777.
[27] C. Marinelli, H. Giberti, and F. Resta, "Conceptual design of a gait simulator for testing lower-limb active prostheses," *16th Int. Conf. Res. Educ. Mechatronics, REM 2015 - Proc.*, pp. 314–320, 2016, doi: 10.1109/REM.2015.7380413.
[28] T. Lenzi, J. Sensinger, J. Lipsey, L. Hargrove, and T. Kuiken, "Design and preliminary testing of the RIC hybrid knee prosthesis," *Proc. Annu. Int. Conf. IEEE Eng. Med. Biol. Soc. EMBS*, vol. 2015-Novem, pp. 1683–1686, 2015, doi: 10.1109/EMBC.2015.7318700.
[29] T. Yu, A. R. Plummer, P. Iravani, J. Bhatti, S. Zahedi, and D. Moser, "The Design, Control, and Testing of an Integrated Electrohydrostatic Powered Ankle Prosthesis," *IEEE/ASME Trans. Mechatronics*, vol. 24, no. 3, pp. 1011–1022, 2019, doi: 10.1109/TMECH.2019.2911685.
[30] J. Zhu, Q. Wang, and L. Wang, "On the design of a powered transtibial prosthesis with stiffness adaptable ankle and toe joints," *IEEE Trans. Ind. Electron.*, vol. 61, no. 9, pp. 4797–4807, 2014, doi: 10.1109/TIE.2013.2293691.
[31] J. J. Rice, J. M. Schimmels, and S. Huang, "Design and evaluation of a passive ankle prosthesis with powered push-off," *J. Mech. Robot.*, vol. 8, no. 2, pp. 1–8, 2016, doi: 10.1115/1.4031302.
[32] H. M. Herr and A. M. Grabowski, "Bionic ankle-foot prosthesis normalizes walking gait for persons with leg amputation," *Proc. R. Soc. B Biol. Sci.*, vol. 279, no. 1728, pp. 457–464, 2012, doi: 10.1098/rspb.2011.1194.

[33] S. K. Au, J. Weber, and H. Herr, “Powered ankle-foot prosthesis improves walking metabolic economy,” *IEEE Trans. Robot.*, vol. 25, no. 1, pp. 51–66, 2009, doi: 10.1109/TRO.2008.2008747.
[34] A. D. Segal *et al.*, “The effects of a controlled energy storage and return prototype prosthetic foot on transtibial amputee ambulation,” *Hum. Mov. Sci.*, vol. 31, no. 4, pp. 918–931, 2012, doi: 10.1016/j.humov.2011.08.005.
[35] J. M. Caputo and S. H. Collins, “A universal ankle-foot prosthesis emulator for human locomotion experiments,” *J. Biomech. Eng.*, vol. 136, no. 3, 2014, doi: 10.1115/1.4026225.
[36] M. Kim, T. Chen, T. Chen, and S. H. Collins, “An ankle-foot prosthesis emulator with control of plantarflexion and inversion-eversion torque,” *IEEE Trans. Robot.*, vol. 34, no. 5, pp. 1183–1194, 2018, doi: 10.1109/TRO.2018.2830372.
[37] P. Malcolm, R. E. Quesada, J. M. Caputo, and S. H. Collins, “The influence of push-off timing in a robotic ankle-foot prosthesis on the energetics and mechanics of walking,” *J. Neuroeng. Rehabil.*, vol. 12, no. 1, 2015, doi: 10.1186/s12984-015-0014-8.
[38] F. Sup, A. Bohara, and M. Goldfarb, “Design and control of a powered transfemoral prosthesis,” *Int. J. Rob. Res.*, vol. 27, no. 2, pp. 263–273, 2008, doi: 10.1177/0278364907084588.
[39] T. Lenzi, M. Cempini, L. Hargrove, and T. Kuiken, “Design, development, and testing of a lightweight hybrid robotic knee prosthesis,” *Int. J. Rob. Res.*, vol. 37, no. 8, pp. 953–976, 2018, doi: 10.1177/0278364918785993.
[40] diah gayatri Arumaningrum, “Asymmetric Unilateral Transfemoral Prosthetic Simulator,” *Lincolin Arsyad*, vol. 3, no. 2, pp. 1–46, 2014, [Online]. Available: http://journal.stainkudus.ac.id/index.php/equilibrium/article/view/1268/1127.
[41] T. Natsakis, J. Burg, G. Dereymaeker, I. Jonkers, and J. Vander Sloten, “Inertial control as novel technique for in vitro gait simulations,” *J. Biomech.*, vol. 48, no. 2, pp. 392–395, 2015, doi: 10.1016/j.jbiomech.2014.11.044.
[42] R. Allemang, J. De Clerck, C. Niezrecki, and A. Wicks, “Special Topics in Structural Dynamics, Volume 6: Proceedings of the 31st IMAC, A Conference on Structural Dynamics, 2013,” *Conf. Proc. Soc. Exp. Mech. Ser.*, vol. 6, pp. 35–45, 2013, doi: 10.1007/978-1-4614-6546-1.
[43] J. Zhang, L. Shen, L. Shen, and A. Li, “Gait analysis of powered bionic lower prosthesis,” *2010 IEEE Int. Conf. Robot. Biomimetics, ROBIO 2010*, pp. 25–29, 2010, doi: 10.1109/ROBIO.2010.5723297.
[44] J. H. Kim and J. H. Oh, “Development of an above knee prosthesis using MR damper and leg simulator,” *Proc. - IEEE Int. Conf. Robot. Autom.*, vol. 4, pp. 3686–3691, 2001, doi: 10.1109/ROBOT.2001.933191.
[45] J. Thiele, S. Gallinger, P. Seufert, and M. Kraft, “The gait simulator for lower limb exoprostheses – Overview and first measurements for comparison of microprocessor controlled knee joints,” *Facta Univ. Ser. Mech. Eng.*, vol. 13, no. 3, pp. 193–203, 2015.
[46] A. J. Van Den Bogert, T. Geijtenbeek, O. Even-Zohar, F. Steenbrink, and E. C. Hardin, “A real-time system for biomechanical analysis of human movement and muscle function,” *Med. Biol. Eng. Comput.*, vol. 51, no. 10, pp. 1069–1077, 2013, doi: 10.1007/s11517-013-1076-z.
[47] D. A. Winter, *Biomechanics and Motor Control of Human Movement: Fourth Edition*. 2009.
[48] A. Naveed, M. H. Ahmed, U. Fatima, and M. I. Tiwana, “Design and Analysis of Dynamic Energy Return Prosthesis Foot using Finite Element Method,” pp. 1–5, 2016,

doi: 10.1109/IHMSC.2016.138.
[49] A. Vitali, C. Rizzi, and D. Regazzoni, “Design and Additive Manufacturing of Lower Limb,” *ASME 2017 Int. Mech. Eng. Congr. Expo.*, pp. 1–7, 2017.